Preoperative and Intraoperative Lymphatic Mapping for Radioguided Sentinel Node Biopsy in Cancers of the Male Reproductive System

15

Hielke Martijn de Vries, Joost M. Blok, Hans N. Veerman, Florian van Beurden, Henk G. van der Poel, Renato A. Valdés Olmos, and Oscar R. Brouwer

Contents

15.1 **Introduction** 331
15.2 **Penile Cancer** 332
15.3 **Prostate Cancer** 337
15.4 **Testicular Cancer** 343
Clinical Cases 347
References 354

Learning Objectives

- To learn indications and clinical rationale for the sentinel lymph node (SLN) procedure in penile, prostate, and testicular cancer
- To acquire knowledge on the different techniques to use for lymphatic mapping and SLN visualization in urological malignancies
- To broaden the knowledge about the dissemination routes in cancer of the male reproductive system
- To understand the techniques used to reduce the SLN false-negative rates in penile, prostate, and testicular cancer
- To acquire knowledge about the practical execution and implications of the SLN procedure in penile, prostate, and testicular cancer
- To understand the role of preoperative and intraoperative imaging in the SLN procedure in penile, prostate, and testicular cancer

H. M. de Vries · J. M. Blok · H. N. Veerman · F. van Beurden
H. G. van der Poel · O. R. Brouwer (✉)
Department of Urology, Netherlands Cancer Institute, Amsterdam, Netherlands
e-mail: hm.d.vries@nki.nl; j.blok@nki.nl; h.veerman@nki.nl; f.van.beurden@nki.nl; h.vd.poel@nki.nl; o.brouwer@nki.nl

R. A. Valdés Olmos
Department of Radiology, Section of Nuclear Medicine and Interventional Molecular Imaging Laboratory, Leiden University Medical Center, Leiden, The Netherlands
e-mail: r.a.valdes_olmos@lumc.nl

15.1 Introduction

The SLN procedure, including preoperative lymphatic mapping, has become an essential component of lymph node staging in penile cancer. The extensive experience with sentinel lymph node biopsy (SLNB) in this cancer has led to an increasing application of the procedure for other urological malignancies. Although both preoperative lymphatic mapping and intraoperative SLN detection are common parts of the urological applications, injection techniques for tracer administration and lymphatic drainage patterns may differ for the different cancers. In penile cancer, lymphatic drainage is mainly superficial, the first draining lymph nodes are usually located in the groin, and the biopsy is performed by means of open surgery. In con-

G. Mariani et al. (eds.), *Atlas of Lymphoscintigraphy and Sentinel Node Mapping*,
https://doi.org/10.1007/978-3-030-45296-4_15

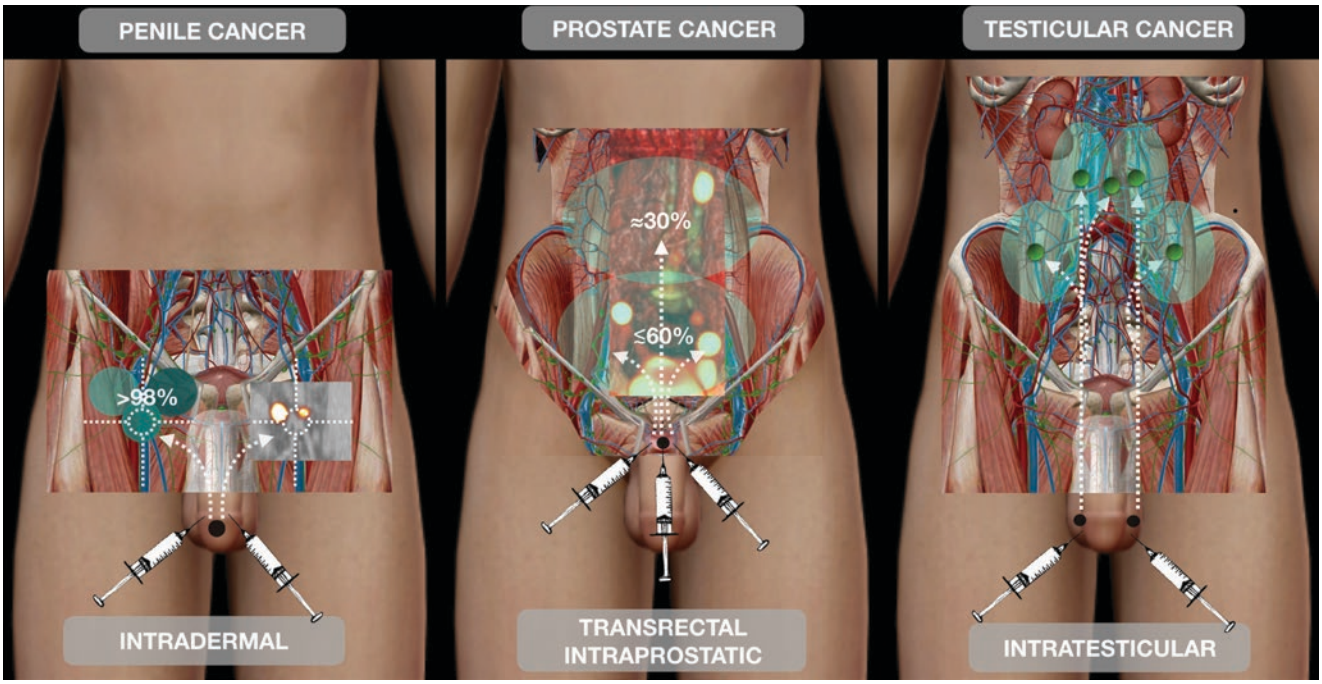

Fig. 15.1 Schematic illustration of tracer injection and areas of SLN drainage in urological malignancies. For penile cancer (on the left) radiotracer is superficially injected and drainage is mostly bilateral with >98% SLNs located in the upper and central inguinal Daseler's areas, especially the inner superior quadrant (dark green circle) [28]; this is illustrated by a superimposed coronal SPEC/CT in the left groin. For prostate cancer (middle) after deep tracer injection drainage is multidirectional with approximately 60% of the SLNs along the internal iliac vessels, obturator fossa, and external iliac vessels; in almost 19% there is direct drainage to lymph nodes above the common iliac bifurcation and 10% above the aorta bifurcation [52, 53]; this is illustrated by a superimposed coronal volume-rendered SPECT/CT. In testicular cancer (on the right) following injection in the left testicle drainage to retroperitoneal para-aortic SLNs is mostly seen whereas after injection in the right testicle both paracaval and interaortocaval lymphatic drainage is expected; less frequently, SLNs are observed along the testicular vessels [71]

trast, in prostate cancer radiotracer migration from the injection site mostly concerns SLNs along the iliac vessels, and other deep-located lymphatic areas, which are resected by (robot-assisted) laparoscopy. In testicular cancer the most frequent drainage route is retroperitoneal along the aorta or vena cava inferior and SLNs are removed using laparoscopy. Some differences in radiotracer administration and lymphatic drainage for penile cancer, prostate cancer, and testicular cancer are illustrated in Fig. 15.1 and further in this chapter the principles of lymphatic mapping and SLNB for these urological malignancies are described.

15.1.1 Tracer Development: Hybrid Radio- and Fluorescence-Guided Approaches

Among other advances in recent years, combined fluorescence- and radioguided approaches such as the hybrid tracer indocyanine green (ICG)-^{99m}Tc-nanocolloid have been introduced during SLN procedures for penile and prostate cancer [1] in the Netherlands and other European countries. This hybrid nanocolloid has both fluorescence and radiologic properties. Adding the fluorescent moieties does not alter the biological properties of the parental radiocolloid, and it enables intraoperative near-infrared fluorescence imaging of the exact same (radioactive) lymph nodes which are preoperatively identified by lymphoscintigraphy and SPECT/CT [2]. ICG absorbs light in the near-infrared spectrum, mainly between 600 and 900 nm, and emits fluorescence between 750 and 950 nm, which can be detected by a fluorescence camera allowing real-time visual guidance during surgery [1]. It is prepared by adding pertechnetate to a vial of nanocolloid (GE Healthcare, Eindhoven, The Netherlands). ICG (PULSION Medical, Feldkirchen, Germany) is added and the content of the vial is subtracted in a syringe after which saline is added to reach a specified volume [3].

15.2 Penile Cancer

Penile cancer is a relatively rare disease in the Western world, with an incidence of approximately 1 per 100,000 [4]. Nearly all penile malignancies are squamous cell carcinomas. The presence of lymph node involvement is the single most

important prognostic factor for cancer-specific death and warrants a poor cancer-specific survival of 80%, 66%, or 37%, respectively, for N1, N2, or N3 disease [5, 6]. Likewise, distant metastases without lymph node metastases are extremely rare. Since the introduction of an anatomically based SLN procedure in penile carcinoma by Cabañas et al. in 1977, the procedure has evolved into a reliable dynamic staging technique, with a low complication rate (7.6–21.4%) compared to (prophylactic) inguinal lymphadenectomy (ILND) (24–58%) [7–13].

15.2.1 The Clinical Problem

Penile cancer patients are divided into two subgroups: patients with (cN+) or without (cN0) palpable inguinal nodes. Patients that are staged cN+ have nodal metastases in 60–80% of cases [14], while cN0 patients have nodal metastases in 13–16% [14]. Initially, for the best chance of cure, ILND was performed directly in all patients [15]. However, this leads to an overtreatment in more than 80% of the cN0 patients. Furthermore, the morbidity (such as lymphedema and infection) of ILND had decreased in the past years but remains, nevertheless, substantial. As currently available noninvasive staging techniques lack sufficient accuracy, minimally invasive staging remains necessary for the time being. Initially, the SLN procedure for penile cancer had a high false-negative rate after its clinical introduction in 1994. After analysis of false-negative cases, several modifications were made to the dynamic SLNB procedure, which increased its sensitivity from 79 to 94% [7, 9, 16, 17]. For these reasons, the EAU and NCCN guidelines of 2018 both recommend the SLN procedure (in expert centers) for cN0 patients [18, 19].

15.2.2 Indications and Contraindications for SLNB

According to the guidelines patients with ≥T1G2 tumors and cN0 groins defined by palpation are eligible for SLNB. However, a preoperative negative ultrasound with fine-needle cytology of suspicious nodes (US ± FNAC) is strongly advised to reduce false negatives due to, e.g., tumor blockage [20]. Studies have also safely included cN+ patients with a negative US ± FNAC or cN+ patients where the suspicious nodes on ultrasound were also removed [21, 22]. Repeat SLNB after tumor recurrence is also a validated procedure [11, 23, 24]. If the SLN is tumor positive, radical ipsilateral lymphadenectomy is performed. In 80% of patients, no additional metastases are found at ILND after a positive SLNB [25]. However, currently no other treatment options are available for this group. Groins with tumor-free SLNs are managed with close surveillance, thereby avoiding the morbidity associated with lymphadenectomy.

15.2.3 Radiocolloid and Modalities of Injection

The tracer (^{99m}Tc-nanocolloid in most European countries) is injected intradermally. In fact, subcutaneous administration is easier to accomplish, but may not accurately identify the route of drainage from an overlying cutaneous site. Furthermore, lymphatic drainage from the dermis is much faster than drainage from subcutaneous tissue. Application of a spray containing xylocaine 10% 30 min before tracer administration is recommended. As an alternative, a lidocaine/prilocaine-based crème can be used. This local anesthesia ensures that the radiocolloid injections are well tolerated and relatively easy to perform. A volume of 0.2–0.4 mL containing 50–90 MBq divided into three depots (0.1 mL each) is subsequently administered intradermally. Each depot is injected raising a bleb. The radiocolloid is injected proximally from the tumor. For large tumors not restricted to the glans, the radiocolloid can be injected in the prepuce. Injection margins within 1 cm from the primary tumor are recommended. A reproducibility rate of 100% for penile lymphoscintigraphy has been reported with an injection distance of 5 mm [26]. In patients with a previous excision biopsy scar, a secondary SLN procedure can be performed by administrating injections using similar margins. Recently, Winter et al. reported the first application of superparamagnetic iron oxide nanoparticles in a patient using MRI for preoperative SLN mapping and a handheld magnetometer for the intraoperative procedure [27].

15.2.4 Preoperative Imaging of SLNs

Lymphoscintigraphy after radiocolloid injection consists of two phases: (a) Dynamic scintigraphy, performed during the first 10 min after radiocolloid injection, preferably in both the anterior and lateral views: The dynamic study is helpful to identify lymphatic ducts and the first directly draining lymph nodes. (b) Static planar imaging at 20–30 min and at 2 h: The early planar images visualize the first draining lymph nodes in about 77–95% of the cases [8, 21, 22, 28]. On SPECT/CT visualization is seen in 90–97% of groins [21, 22, 28]. Immediate or delayed (a few weeks later) radiocolloid reinjection or additional images at 4 h are recommended when no SLNs are visualized [8]. If still no visualization is seen exploration of the groin is an option and

in low-risk patients (<pT1G3) close clinical surveillance with ultrasound can be considered [29]. Generally, the lymph nodes draining directly from the injection site are classified as SLNs. The first node appearing in a basin is considered to be the SLN in case of multiple visible nodes without visible afferent vessels.

15.2.5 Lymphatic Drainage

The most frequently visualized lymphatic drainage pattern is bilateral drainage to both groins (80%) (Fig. 15.2). This pattern is, however, asynchronous in two-thirds of cases, and often visualization of the contralateral lymph nodes is only possible on delayed imaging [30]. Drainage from the injection site mostly occurs through one or two visualized afferent lymphatic ducts leading to one or two SLNs in each groin. In some cases a cluster of inguinal lymph nodes is observed. After drainage to both groins, drainage through the node of Rossemüller-Cloquet, on the interface of the groin and pelvis, into the iliacal and obturator nodes is seen. These are almost always second-echelon nodes. Crossover drainage from the groin to the contralateral pelvis has never been seen.

15.2.6 Intraoperative Detection of SLNs

It is safe to perform surgery on the day or the day after injection and nodal imaging [11]. There are indications that the 1-day protocol has higher radioactive count, more nodes, and more morbidity [11].

As is customary for SLNB in melanoma and breast cancer, intraoperative SLN detection is guided by a gamma ray detection probe and blue dye or indocyanine

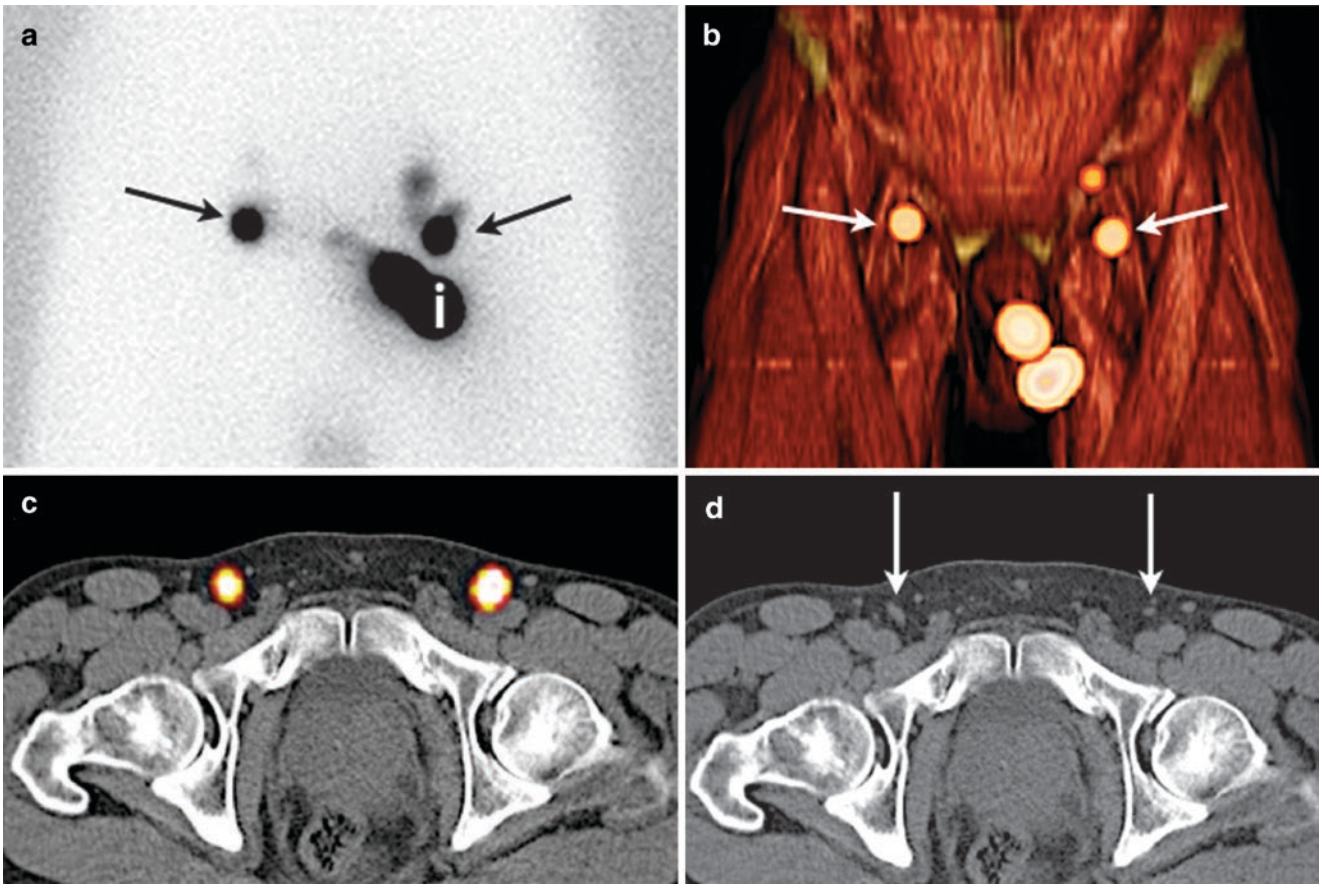

Fig. 15.2 A 49-year-old patient with penile squamous cell carcinoma scheduled for partial penectomy and SLNB. (**a**) Lymphoscintigraphy 2 h after injection of 81 MBq ^{99m}Tc-nanocolloid (i) shows drainage to a SLN in both groins (arrows) and bilateral higher echelon drainage. (**b**) 3D volume-rendered SPECT/CT image revealing that both SLNs are located in the central zone of Daseler. (**c**, **d**) Axial fused SPECT/CT images depicting both radioactive SLNs with the corresponding lymph nodes on CT (arrows)

green (ICG). After excision of all preoperatively defined SLNs, it is important to carefully search for any residual radioactivity using the probe and if available a portable gamma camera, to prevent that any remaining/additional SLNs are left behind [31, 32]. Furthermore, intraoperative palpation of the wound should take place to identify suspicious lymph nodes that failed to pick up any radiocolloid [33].

15.2.7 Contribution of SPECT/CT

SPECT/CT images are usually acquired after the 2-h planar images, and contribute to a better understanding of the location of the SLNs in penile carcinoma (Figs. 15.2 and 15.3). SPECT/CT enables the anatomical localization of the SLNs that were previously identified by lymphoscintigraphy. For instance, the modality can differentiate inguinal from iliac (most frequently second-echelon) lymph nodes. Moreover, SPECT/CT enables visualization of the SLNs in the so-called Daseler's superior and central inguinal zones that are superior to and directly overlying the saphenofemoral junction, respectively. SPECT/CT has confirmed that in the majority of patients SLNs are found in the superior medial (30–73%), in the superior lateral (9–37%), and in the central zones (18–32%) [28]. Lymphatic drainage to the inferior quadrants is rare (inferior medial 1.6%, inferior lateral 0%) [28]. SPECT/CT identifies SLNs in groins which

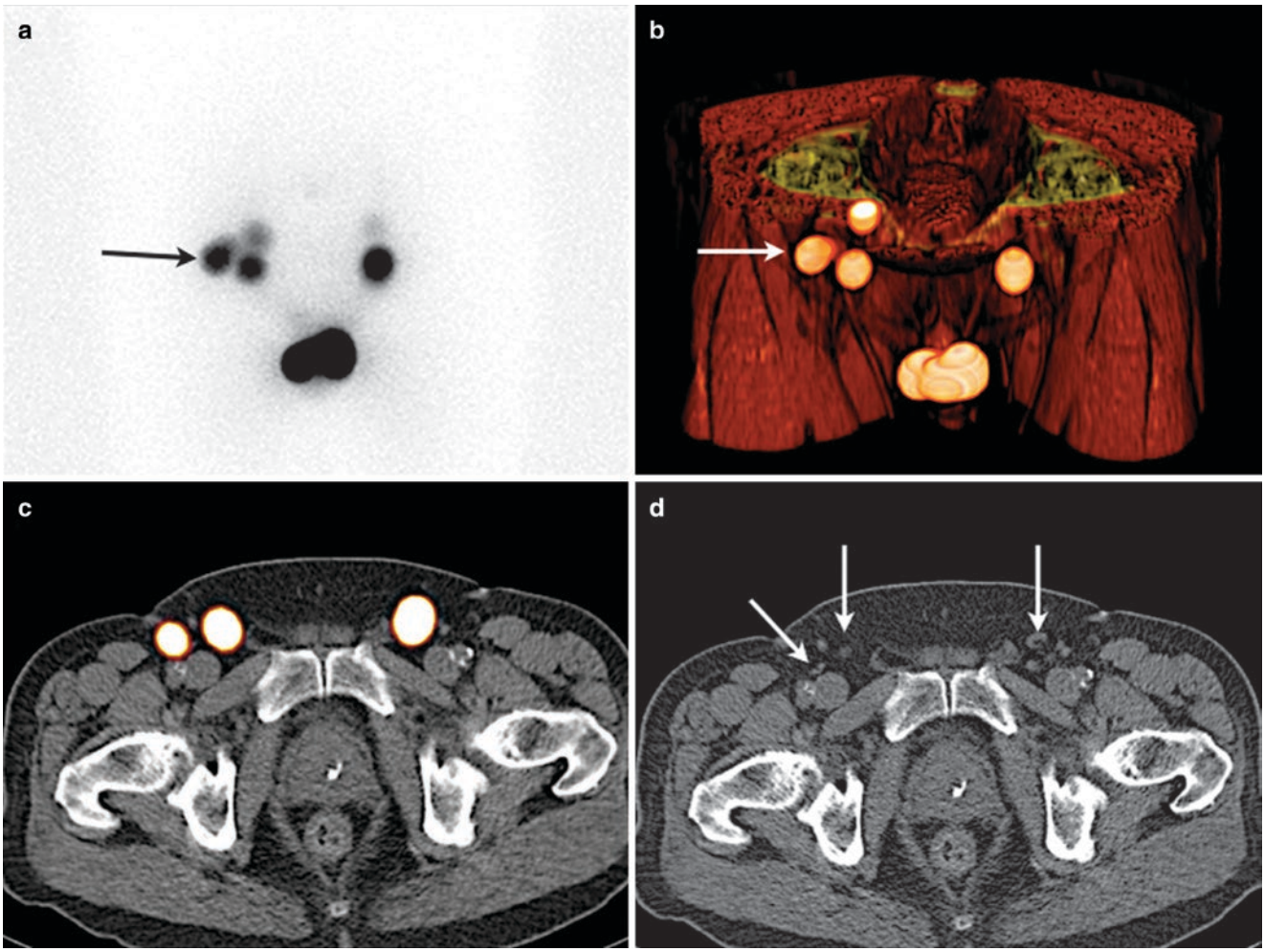

Fig. 15.3 (**a**) Intradermal injection of 82.92 MBq ^{99m}Tc-nanocolloid in a 71-year-old male resulting in visualization of a SLN in both groins with a second more laterally localized SLN on the right side (arrow) on delayed planar lymphoscintigraphy. (**b**) 3D volume-rendered SPECT/CT images revealing a SLN in the superior medial quadrant on both sides, and a SLN in the superior lateral quadrant on the right side (arrow). The image also shows a second-echelon node in the right iliac area. (**c**, **d**) Axial fused SPECT/CT images depicting both radioactive SLNs with the corresponding lymph nodes on CT (arrows). Histopathological examination revealed micrometastases in the left excised SLN

would have had non-visualization if only conventional lymphoscintigraphy had been used [34, 35]. Finally, SPECT/CT is able to identify contamination of the skin with the radiocolloid, an occurrence which can sometimes be erroneously interpreted as lymph nodes on planar lymphoscintigrams.

15.2.8 Intraoperative Imaging

Accurate staging with SLNB can be achieved only if all nodes on a direct drainage pathway from the tumor are harvested. If SLNs are left behind, this constitutes one of the potential causes for false-negative results. The integration of a portable gamma camera in the intraoperative procedure may increase the detection sensitivity, as it provides an intraoperative overview image of the radioactive SLNs and enables post-excision confirmation of complete removal of the SLNs in the operating room. For optical visualization of the SLN, vital blue dyes are traditionally used to stain 43–56% of nodes [8, 32, 36]. To increase intraoperative visualization rate, ICG-^{99m}Tc-nanocolloid can be utilized as mentioned in the second paragraph [37]. With this combined tracer, 95–97% of the removed SLNs were fluorescent in vivo [32, 36]. These developments may help to further refine intraoperative retrieval of SLNs.

15.2.9 Common and Rare Variants

One of the advantages of lymphatic mapping is its ability to identify SLNs outside the usual nodal basins. In penile cancer, direct drainage to prepubic SLNs has been described [38]. In particular, dynamic lymphoscintigraphy often shows one or two lymphatic vessels leading to the SLNs. Such vessels have also been observed to directly lead to deep inguinal and even to iliac SLNs.

Blockage of the lymph flow by tumor metastasis in the lymph node may cause non-visualization and lymph rerouting with occasionally retrograde or contralateral flow of the ^{99m}Tc-nanocolloid. This occurrence has been visualized by SPECT/CT imaging [33].

15.2.10 Technical Pitfalls

The most frequent pitfall is skin contamination. The high pressure of the intradermal bleb can result in leakage during injection or after removal of the needle. The use of (surgical) lights to adequately visualize the site of injection and of a fenestrated drape to cover the area may help to avoid skin contamination. Furthermore, voiding of radioactive urine between the early and delayed scintigraphy may also cause skin contamination. The hot spots due to skin contamination may be confused with SLNs, thus leading to an unnecessary intraoperative pursuit. In these cases skin decontamination is mandatory. Complementary SPECT/CT may also be helpful in detecting these artifacts. Another possible pitfall is accidental injection into the corpus cavernosum, an occurrence that will cause no visualization of lymphatic flow. Furthermore, in some cases the injection site (penis) may obscure visualization of the more inferiorly located SLNs on anterior planar imaging.

15.2.11 Accuracy of Radioguided SLNB

Initially, the most significant drawback of SLNB for penile cancer was a relatively high false-negative rate (22%) [39]. After analysis of the false-negative cases, several modifications were made to decrease the false-negative rate [9]. Histopathologic analysis was expanded with serial sectioning of the SLNs. Furthermore, preoperative ultrasonography of cN0 groins with fine-needle aspiration cytology (FNAC) of suspicious lymph nodes was added, as well as exploration of groins in case of non-visualization during scintigraphy and intraoperative palpation of the wound to identify suspicious lymph nodes that failed to pick up any radiocolloid. Thanks to these modifications, the procedure has evolved into a reliable minimally invasive staging technique with an associated sensitivity of 93–95% with low morbidity in experienced centers [9, 40]. At the same time the SLN procedure has also increased survival of penile cancer patients significantly [6, 41]. However, a recent multicenter meta-analysis reported pooled sensitivity rates of 88% [17, 42]. One explanation for such lower sensitivity may be represented by differences in protocols (that is, screening with ultrasound and FNAC to detect lymph node metastases that fail to pick up radioactivity), low-volume centers, and/or possibly different phases of the learning curve.

Key Learning Objectives Penile Cancer

- The SLN procedure in penile cancer has helped increase survival and prevents unnecessary lymphadenectomy in patients with a tumor-negative SLN.
- The SLN procedure in penile cancer can be performed in a 1- or 2-day protocol.

- SLNB after primary tumor excision is also possible and can be performed in a similar fashion.
- Repeat SLNB for penile cancer recurrence is safe.
- SPECT/CT provides anatomical information giving specific landmarks for SLN localization during the surgical act.

15.3 Prostate Cancer

In prostate cancer, lymph node staging is important for both prognosis and therapeutic management. The presence of lymph node metastases may lead to adjuvant treatment in case of prostatectomy, such as hormonal therapy with or without radiotherapy, or extension of the radiotherapeutic field [43]. To date, none of the available noninvasive diagnostic imaging modalities provide a reliable assessment of lymph node (micro)metastases. Positron-emission tomography (PET) with prostate-specific membrane antigen (PSMA) labeled with ^{68}Ga or ^{18}F is an emerging imaging modality; however, the sensitivity for detection of lymph node metastases is still limited to 64% in the case of ^{68}Ga-PSMA PET/CT. Moreover, ^{68}Ga-PSMA PET/CT has been found not to detect lymph node metastases smaller than 2 mm [44, 45]. Therefore, surgical staging by extended pelvic lymph node dissection (ePLND) is still the current standard of care. However, SLNB is emerging as an alternative staging method, with a lower incidence of complications and with the potential to identify relevant lymph nodes outside the standard ePLND field [46, 47].

15.3.1 The Clinical Problem

Current international guidelines recommend that a pelvic lymph node dissection (PLND) should be performed at the time of a radical prostatectomy (RP) in all men with intermediate- or high-risk prostate cancer, if the estimated risk of lymph node metastases exceeds 5% in the current EAU guidelines or 2% with NCCN guideline nomograms (grade recommendation: "B"). Despite this, 25–35% of the PC patients who are treated with curative intent with RP and extended PLND will develop clinically significant biochemical recurrence with local and/or distant disease. An extended dissection (ePLND) is preferred over limited PLND. However, even with an extended dissection template including external iliac, hypogastric, and obturator nodes, 35% of lymph nodes potentially containing PC will not be removed at surgery, either being located out of the standard surgical field or being missed within.

The advantages of SLN dissection are the possibility to identify tumor draining lymph nodes outside the field of an ePLND and lower the incidence of complications compared to ePLND [46]. However, accurate localization of SLNs in the pelvis can be challenging, especially when SLNs are located near the prostatic injection site (because of the high radioactive background signal), or in case of aberrantly located SLNs (e.g., para-aortic) [48].

15.3.2 Indications and Contraindications for SLNB

The probability of having lymph node metastasis from prostate cancer increases with the serum level of prostate-specific antigen (PSA), biopsy grade (Gleason score), and clinical T stage. Like the indications for an ePLND, SLNB could be performed in all men with intermediate- and high-risk prostate cancer, if the estimated risk of lymph node metastases exceeds 5% with EAU guidelines or 2% with NCCN guideline nomograms and PSMA PET/CT or any other conventional imaging modality showed no evidence of lymph node metastases. However, according to the guidelines, due to lack of reliable evidence regarding oncological effectiveness, SLNB is still an experimental nodal staging procedure. A tumor-bearing SLN may influence the boundaries of the radiotherapy field and duration of hormonal (androgen deprivation) therapy. Another possible indication is to select patients who are eligible for salvage treatment of the prostate, as the usual parameters to stratify patients in risk groups do not apply to patients with intraprostatic recurrence [49]. Since salvage treatment of the prostate may result in serious complications, it is considered when the prostate is actually the only tumor-bearing site.

15.3.3 Radiocolloid and Modalities of Injection

Most of the experience in the SLN procedure for prostate cancer has been acquired in European countries and the most frequently used radiopharmaceutical has been ^{99m}Tc-nanocolloid. Transrectal intraprostatic injection is guided by (transrectal) ultrasound, injecting the radiocolloid under continuous monitoring using a needle of 0.5 × 150 mm (Fig. 15.4). Prostate cancer may be multifocal; therefore injections are performed in both lobes. An activity of about 240 MBq in 0.4 mL is recommended. The lymph node visu-

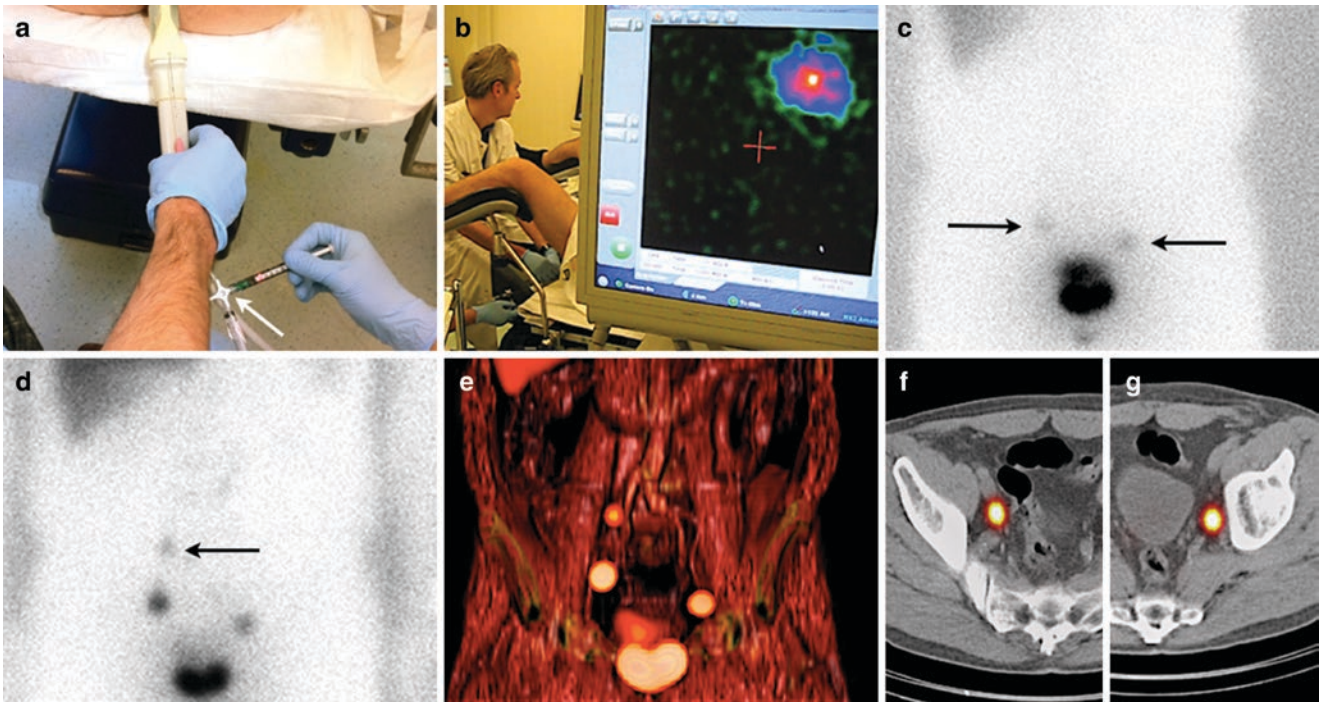

Fig. 15.4 Preoperative SLN mapping in a 65-year-old patient with intermediate-risk prostate cancer. (**a**) Tracer administration guided by transrectal ultrasound guidance using a long needle and a three-way system. (**b**) The radioactive dose is divided into 2–4 injections. The procedure is monitored using a portable gamma camera to verify adequate tracer retention within the prostate. (**c**) Early planar lymphoscintigram showing two SLNs with direct drainage from the prostate (arrows). (**d**) The delayed lymphoscintigram enables differentiation of the SLNs and a higher echelon lymph node (arrow). (**e**) 3D volume-rendered SPECT/CT image displaying the location of the SLNs in more detail. (**f**) Axial fused SPECT/CT image showing the SLN on the right side along the external iliac veins and the SLN on the left side (**g**) in the obturator fossa

alization rate tends to be less optimal when lower activities are used. The particle concentration also appears to be important, and the use of a reduced labeling dilution volume (0.4 mL ^{99m}Tc per 0.2 mg nanocolloid) yields more visualized SLNs with higher radioactivity count rates [50]. The radiocolloid is divided into 2–4 injections depending on the prostate volume. A three-way system is recommended, and after each depot saline is used for flushing the residual radioactivity in the needle. When using ICG-^{99m}Tc-nanocolloid a similar injection scheme is applied with a volume of 2.0 mL and an activity of 300 MBq (Fig. 15.5).

15.3.4 Preoperative Imaging of SLNs

In the pelvis, lymphatic ducts are seldom visualized and the relatively slower deep lymphatic drainage renders dynamic lymphoscintigraphy less useful. Early planar images of lymphoscintigraphy acquired 15 min after radiocolloid administration can visualize the first draining lymph nodes in almost 88% of the cases [51]. Delayed imaging may be performed 2–4 h after injection. On delayed imaging the lymph node visualization rate increases to more than 95%. Comparing the early and delayed images enables to differentiate second-echelon lymph nodes from the first draining nodes. This discrimination is based on the anatomical lymph node basins of the pelvis. As a rule, late-appearing lymph nodes located higher in the same basin are considered as second-echelon lymph nodes. Late-appearing lymph nodes in distal or more ventral and dorsal basins suggest direct draining from the prostate. These lymph nodes may also be considered as SLNs. If no SPECT/CT is available, lateral planar images can differentiate between dorsal and more ventral located SLNs.

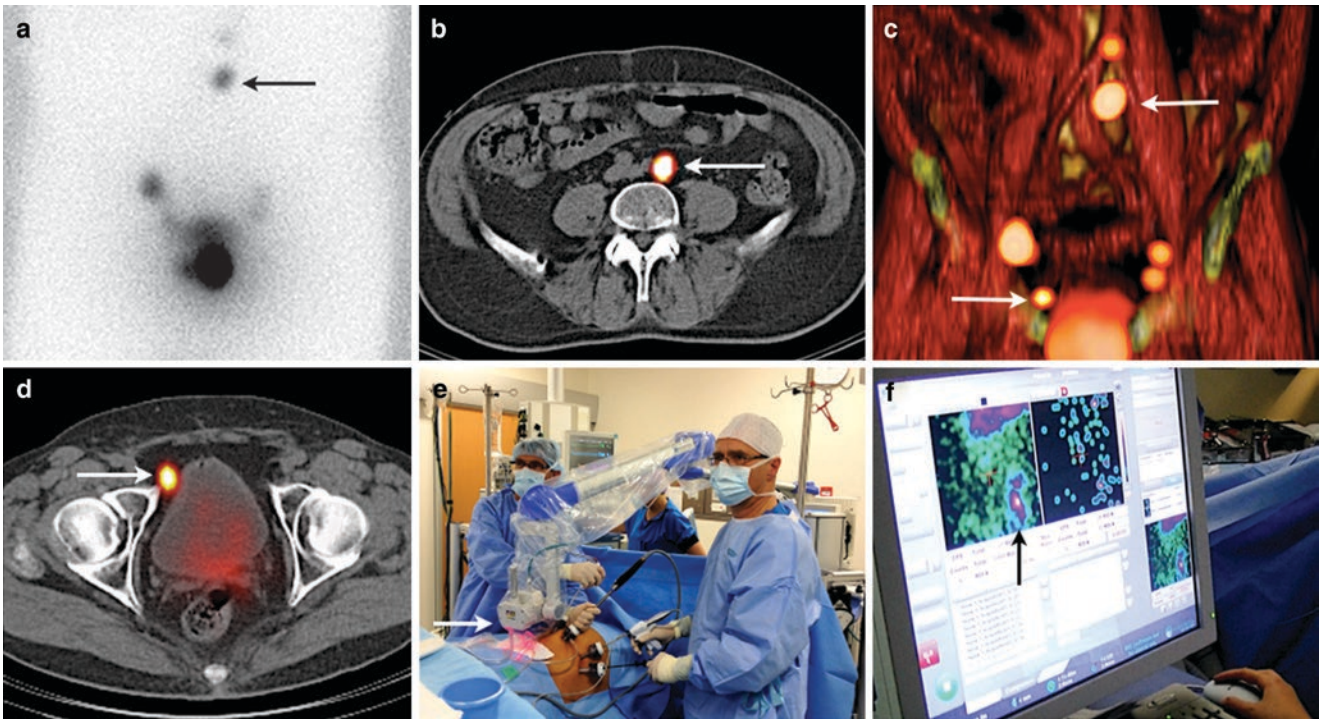

Fig. 15.5 (**a**) Early lymphoscintigraphy after transrectal intraprostatic injection of ^{99m}Tc-nanocolloid (170 MBq) in a 70-year-old male scheduled for SLNB resulted in visualization of bilateral lymphatic drainage with an early-appearing SLN along the great abdominal vessels (arrow). (**b**) Axial SPECT/CT image showing the exact location of this SLN next to the common iliac artery. (**c**) The 3D volume-rendered SPECT/CT image providing an overview of all SLNs: the upper SLN next to the common iliac artery (upper arrow), two along the external iliac vessels on the left side, one along the external iliac artery on the right side, but also an additional SLN located more mediocaudally (lower arrow). (**d**) The axial image shows that this SLN is located paravesically. (**e**) All SLNs were harvested laparoscopically aided by a portable gamma camera (arrow) and a laparoscopic gamma probe. (**f**) Intraoperative visualization of a SLN (arrow) using a portable gamma camera allowing post-excision confirmation that the SLN has been removed completely. After excision (right on screen), no significant remaining activity is seen

15.3.5 Lymphatic Drainage

The lymphatic drainage pathways of the prostate are highly variable in individual patients. Lymph node mapping studies [52, 53] using SPECT/CT, lymphoscintigraphy, SLN procedures, and lymph node dissections improved our understanding of lymphatic drainage. Main drainage pathways include the internal iliac nodes, obturator nodes, and external iliac nodes (Fig. 15.1). These regions are included in the extended pelvic lymph node dissection (ePLND). The borders of the internal iliac nodes are the bifurcation of the internal and external iliac arteries, pelvic floor, bladder wall, and medial to obturator nerve. The obturator region is found lateral to obturator nerve and medial to external iliac artery. The external iliac nodes are found cranial to inguinal ligament, medial to genitofemoral nerve, medial to psoas muscle, and caudal to ureter and bifurcation of internal and external iliac arteries. Less frequently, metastasis is found in the distal or proximal (divided by the ureteric crossing) common iliac artery nodes with the following borders: bifurcation of the aorta (cranial), bifurcation of the internal and external iliac nodes (caudal), internal iliac artery (medial), and genitofemoral nerve and psoas muscle (lateral). The borders of the presacral regions are the common iliac arteries (cranial/lateral), bifurcation of the internal and external iliac arteries (caudal), and promontorium and proximal sacrum (dorsal). These regions are included in the "super-extended PLND." Other rare variants are discussed below.

15.3.6 Intraoperative Detection of SLNs

Initial validation of SLNB in prostate cancer is based on open surgery and use of a gamma ray detection probe to guide detection of the radioactive SLNs. Performing SLNB

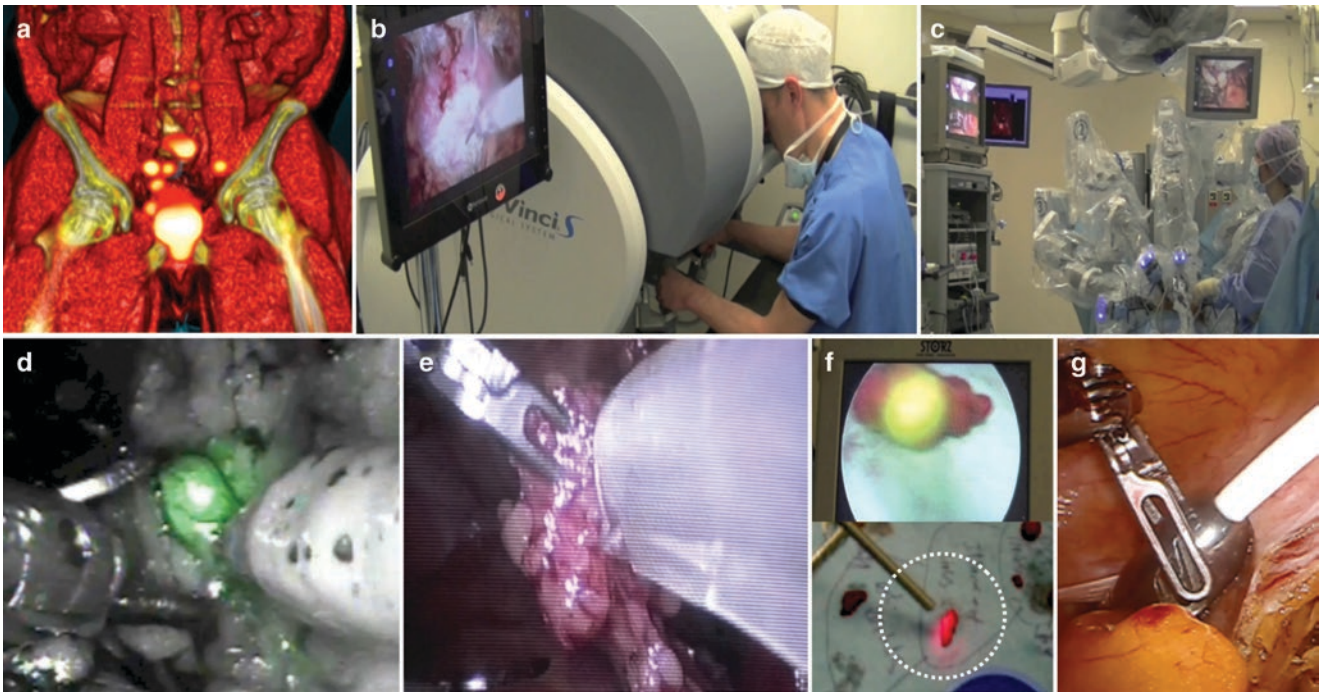

Fig. 15.6 Following administration of the hybrid tracer ICG-^{99m}Tc-nanocolloid, volume-rendered SPECT/CT (**a**) is able to anatomically localize the SLNs in the pelvis. Based on this information, urological surgeons can remove the nodes by means of robot-assisted laparoscopy (**b**, **c**). Thanks to the fluorescence signature of the tracer the SLNs are localized (**d**) and subsequently removed and measured with a rigid laparoscopy gamma probe (**e**). Due to the dual signature of the tracer both fluorescence (top) and radioactivity (circle bottom) can successively be measured (**f**). The replacement of the standard rigid probe by a flexible drop-in gamma probe (**g**) will optimize the procedure in the future

in a robot-assisted laparoscopic setting can be challenging because of the limited maneuverability of gamma ray detection probes. Especially SLNs that lie in close proximity to the injection site are easily missed, because the relatively high background signal from the injection site hinders the localization of the low-intensity signal from the SLN. The introduction of several new technologies has made the incorporation of SLNB in robot-assisted surgery possible [54, 55]. The hybrid tracer ICG-^{99m}Tc-nanocolloid aids in the intraoperative detection of SLNs. However, 14.3–19.6% of SLNs cannot be visualized due to the limited tissue penetration of the ICG fluorescent signal [55]. Those SLNs missed using fluorescence imaging can be localized using preoperatively obtained lymphoscintigraphy and SPECT/CT images and per-operatively with the use of a gamma ray detection probe [54]. Additionally, fluorescence imaging has been incorporated in robotic assisted surgery using a da Vinci Si system with an integrated Firefly fluorescence laparoscope [55]. During the procedure, the urologist can switch between white light imaging and fluorescence imaging using the controllers of the console (Fig. 15.6).

In open surgery, the use of a portable gamma probe aids the detection of SLNs. Current portable gamma cameras are capable of detecting two different signals: the signal of ^{99m}Tc-nanocolloid for SKLN visualization, plus the signal of a ^{125}I seed pointer placed on the tip of the laparoscopic gamma ray detection probe [56]. During surgery the signal of ^{99m}TC, which indicates the location of the SLN, and the signal of ^{125}I seed pointer are both displayed on a screen. The signal of the ^{125}I seed pointer is depicted as a yellow circle, guiding the surgeon spatially to the signal of the SLN. The ^{125}I seed additionally aids in quantifying the amount of radioactivity in the nodes, thus allowing more reliable discrimination between SLNs and second-echelon nodes. After removal of all SLNs, the portable gamma camera can show whether there are any remaining SLNs that have to be removed or a second-echelon node that can confidently be left in place (see Fig. 15.6). This approach provides certainty about completeness of the surgical procedure. The excised lymph nodes are checked for radioactivity with the gamma probe ex vivo.

The use of a drop-in gamma probe in robot-assisted surgery has recently been investigated to overcome the

limited maneuverability of laparoscopic gamma ray detection probes (Fig. 15.6). The drop-in probe is inserted via a trocar and can be maneuvered with laparoscopic surgical tools [57]. This allows placing the drop-in gamma probe in between low-intensity objects (e.g., SN) and high-background objectives like the injection site (e.g., prostate), therewith being able to distinguish signals from low-intensity objects from high-background objectives with a relative intensity ratio of 1:100 [57]. The drop-in probe can remain in the abdominal cavity during the nodal resection and is picked up for placement with the ProGrasp® forceps whenever necessary. A feasibility study showed that the wide scanning range of the drop-in probe allowed the surgeon to remove 35 SLNs in 10 prostate cancer patients. In total, 45% of the SLNs identified with the drop-in probe were considered difficult to trace using the traditional laparoscopic gamma probe [58].

15.3.7 Contribution of SPECT/CT

Hybrid imaging with SPECT/CT enables anatomical localization of SLNs. A 98–99% SLN visualization rate has been reported for SPECT/CT (versus 91% for planar imaging) [52, 53, 59]. Moreover, in 56% of the cases SLNs are localized inside the area of ePLND [52, 53]; there is a considerable number of SLNs in regions not routinely excised when performing an ePLND (see below: accuracy of radioguided SLNB) [47]. SPECT/CT is mostly performed after the delayed planar imaging, and must be interpreted in combination with lymphoscintigraphy. Sequential planar images are able to identify the lymph nodes draining directly from the tumor site, but give only limited information about their anatomical location. With SPECT/CT it is possible to better localize SLNs both inside and outside the pelvis. In many cases early-appearing lymph nodes seen as a single hot spot on planar imaging are displayed as separate lymph nodes in different basins by SPECT/CT, and all of them must be considered as SLNs. In other cases, intense lymph node uptake seen on fused images may correspond to a cluster of SLNs as depicted on the CT component of the SPECT/CT acquisition. As such, SPECT/CT provides valuable information for the urologist, which may lead to a significant shortening of the operation time, as less extensive exploration might be required. Furthermore, SPECT/CT may also provide important information for planning radiotherapy, concerning especially treatment volume and optimization of irradiation fields in the pelvis.

15.3.8 Common and Rare Variants

In prostate cancer, lymphoscintigraphy and SPECT/CT may identify SLNs outside the ePLND in 16–44% of the cases [51–53]. These aberrantly located SLNs can be located in the following regions: common iliac (19%), para-aortic (10%), presacral (7%), aortic bifurcation (4%), pararectal (3%), paravesical (<1%), mesenteric fat (<1%), and inguinal (<1%) [52, 53].

15.3.9 Technical Pitfalls

The relatively complicated radiocolloid injection procedure for prostate cancer is probably the most frequent cause of pitfalls. One must be careful to avoid tracer leakage during injection, possibly resulting in subsequent contamination of the floor or of the ultrasound probe. It is therefore recommended to check for contamination of the room after injection using a Geiger counter.

During injection, incorrect needle placement may result in passage of the radiocolloid directly to the bladder or bloodstream, which in turn may cause non-visualization during scintigraphy. By monitoring the injection procedure with a portable gamma camera, one can ensure adequate radiocolloid retention in the prostate. As the injection is performed transrectally, a possible pitfall is visualization of lymphatic drainage from the rectum, leading to, e.g., visualization of inguinal lymph nodes on SPECT/CT imaging (Fig. 15.7). Furthermore, accidental funicular administration can also occur, possibly leading to retrograde drainage toward the scrotum (Fig. 15.8).

15.3.10 Accuracy of Radioguided SLNB

Original validation of SLNB for prostate cancer was based on open surgery and on the use of a gamma probe to guide detection of the radioactive SLNs. Out of more than 2000 patients evaluated, only 11 false-negative cases (5.5%) were reported [60]. More recently, SLNB has been validated using a laparoscopic gamma probe during minimally invasive surgery [61].

The combined diagnostic accuracy of open, laparoscopic, and robot-assisted SLNB with ePLND as reference standard has been described in a recent systematic review including 2509 patients and showed a 95.2% (81.8–100%) sensitivity, 100% (95.0–100%) specificity, 100% (IQR 87.0–100%) positive predictive value, and 98% (94.3–100%) negative predictive value. In 4.8% (0–18.2%) of cases a metastasis

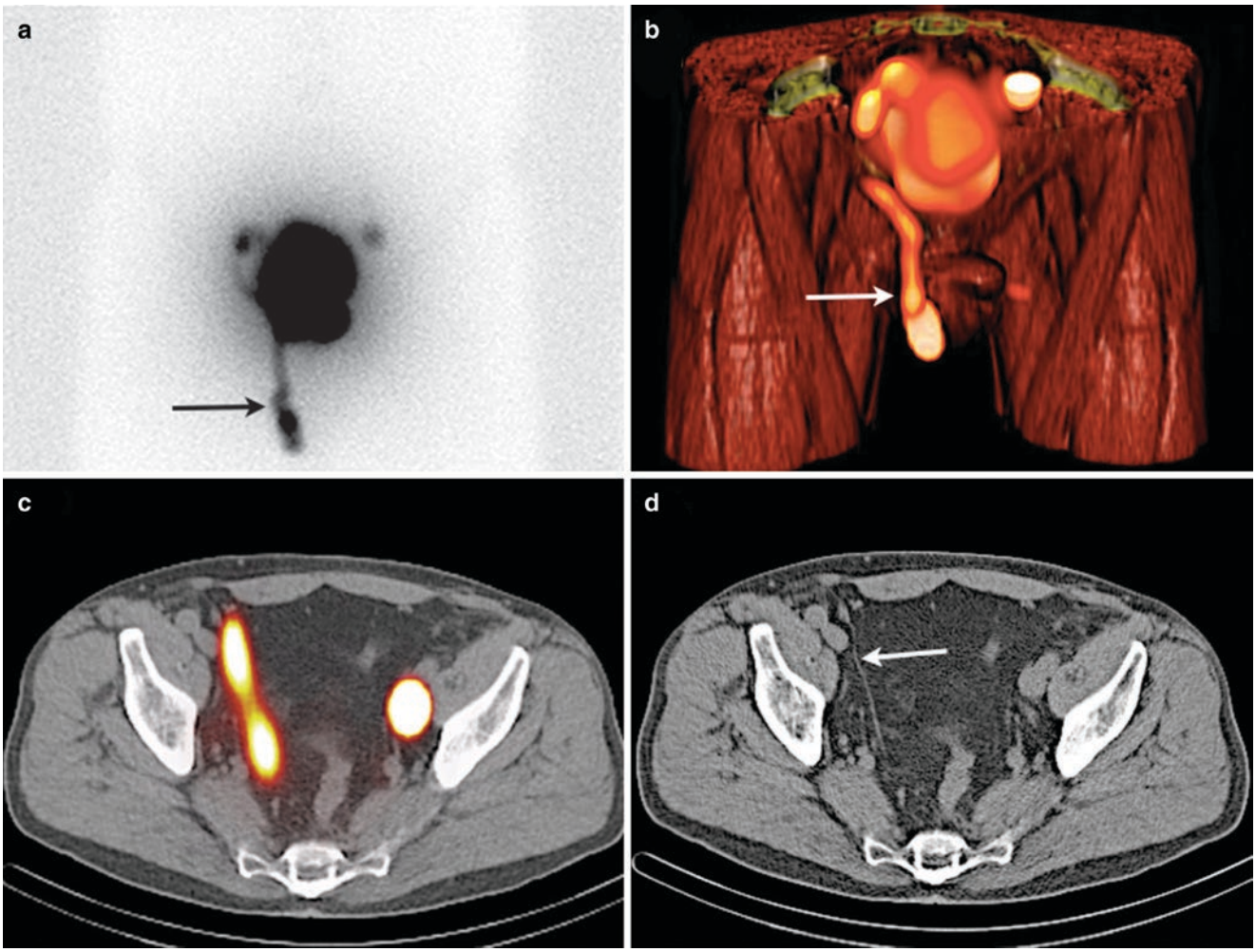

Fig. 15.7 (**a**) Planar lymphoscintigraphy after intraprostatic injection of 180 MBq ^{99m}Tc-nanocolloid in a 60-year-old patient showing bilateral drainage with a single hot spot on both sides, but also with drainage on the right side in caudal direction (arrow). (**b**) 3D volume-rendered SPECT/CT image showing that the caudal drainage on the right side is directed toward the right testicle (arrow). (**c**, **d**) Axial images showing elongated drainage along the funiculus (arrow). The drainage toward the testicle thus reflects retrograde drainage after accidental funicular administration, one of the possible pitfalls of this procedure

was found in the SLN outside the ePLND template without metastasis inside the ePLND template (false positive), suggesting diagnostic advantage and a higher yield of tumor-positive nodes when combining the procedures [47].

Key Learning Points: Prostate Cancer

- Indications for SLN procedure of the prostate are to determine lymph node metastasis in patients with intermediate- and high-risk prostate cancer eligible for radiotherapy with hormonal therapy or patients with prostate cancer eligible for salvage treatment of the prostate.
- With the (new) hybrid tracer ICG-^{99m}Tc-nanocolloid it is possible to perform preoperative imaging with lymphoscintigraphy and SPECT/CT as well as intraoperative imaging with a fluorescence camera and a gamma ray detection probe.
- SLN mapping enables the identification of lymph node metastasis outside the template of extended pelvic lymph node dissection.
- The introduction of drop-in gamma probes may help to overcome the limited maneuverability of rigid laparoscopic gamma probes with advantages especially for robot-assisted SLNB during laparoscopy.

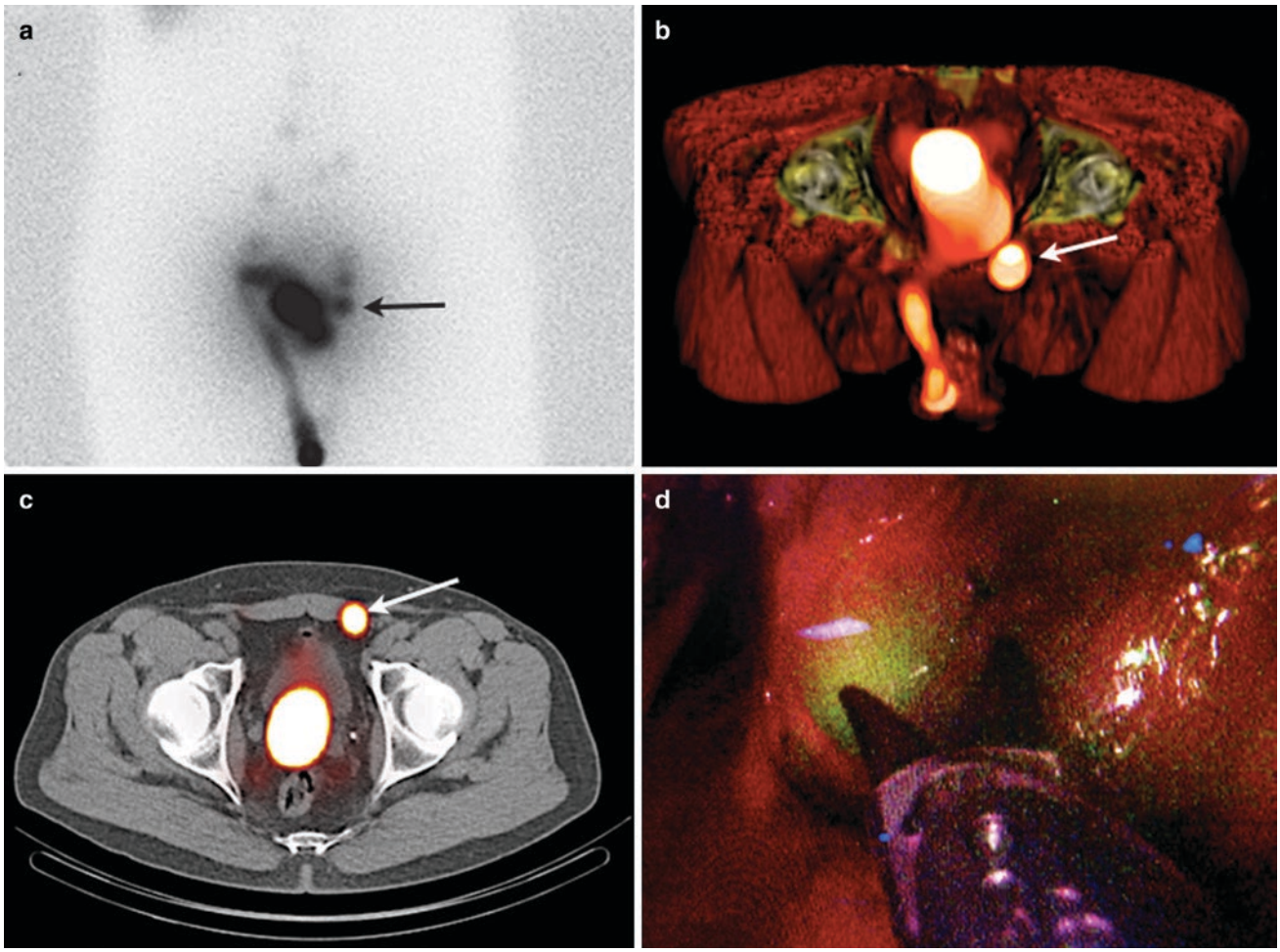

Fig. 15.8 A similar situation arose after transrectal intraprostatic injection (211 MBq) of hybrid radioactive and fluorescent ICG-^{99m}Tc-nanocolloid in a 59-year-old male with intermediate-risk prostate cancer. (**a**) Delayed planar lymphoscintigram showing retrograde drainage toward the scrotum on the right side due to partial funicular tracer administration as well as drainage to SLNs on both sides (obturator fossa); and a SLN located more caudally on the left side (arrow). (**b**, **c**) The 3D volume-rendered and axial SPECT/CT images reveal that the most caudal SLN on the left side reflects aberrant drainage ventrally against the abdominal wall (arrow). The SLNs were harvested during robot-assisted laparoscopy guided by a laparoscopic gamma probe and fluorescence endoscope. (**d**) Fluorescence endoscope image showing the SLN against the abdominal wall along the umbilical ligament (green). This SLN (and an iliac SLN on the right side) contained metastases at histopathology

15.4 Testicular Cancer

Testicular germ cell tumor (TGCT) is the most frequent solid malignancy in young men and affects up to 10 in 10,000 men [62, 63]. Depending on the histologic subtype (seminoma or nonseminomatous germ cell tumor), the peak incidence is between 25 and 35 years old [62]. Incidence rates are rising and increases as high as 4.9% per year have been reported [64]. The prognosis is favorable and cancer-specific survival rates up to 100% have been reported [65–67]. The majority of patients have clinical stage I disease at first presentation [68]. The optimal management of these patients remains controversial. A surveillance policy requires intensive, frequent follow-up visits with costly examinations and defers detection and treatment of lymph node metastases to a later stage. Up to 30% of patients with clinical stage I disease will relapse under surveillance and have to be treated with multiple cycles of toxic chemotherapy. Therefore, there is a need for diagnostic techniques that enable the identification and treatment of patients with occult lymph node metastasis at an earlier stage. In this respect, the SLN procedure is of potential high value [69–71].

15.4.1 The Clinical Problem

Approximately two-thirds of patients present with clinical stage I [68]. The predominant management strategy for these patients is inguinal orchiectomy followed by active surveillance for 5 years [72]. However, 20–30% of patients with clinical stage I will relapse under surveillance [73, 74]. These patients had occult metastatic disease in their lymph nodes at the time of first presentation, undetectable by current imaging protocols or biomarkers.

Patients who suffer from relapse are treated with multiple cycles of platinum-based chemotherapy. These regimens cause serious short- and long-term side effects [75]. For example, the risk of cardiovascular disease or a second malignancy is ~2 times higher after chemotherapy [76]. As a consequence, the relative survival of these patients continues to decline even beyond 30 years of follow-up [77]. For intermediate/poor-risk patients, the treatment-related mortality is even higher than the disease-related mortality.

To overcome the high relapse rate, several risk-adapted strategies have been introduced [78–80]. Risk stratification is based on the outcome of the orchiectomy specimen and high-risk patients receive one cycle of chemotherapy. Approximately 52–68.5% of high-risk patients, however, do not relapse if followed with active surveillance [78, 79, 81]. Thus, treating all high-risk patients with chemotherapy would lead to serious overtreatment. Conversely, 12–14% of low-risk patients will relapse [78, 79, 81]. These patients would have benefitted from adjuvant treatment, but did not receive it.

Thus, the high relapse rate in clinical stage I testicular cancer, the high rate of over- and undertreatment, and the serious morbidity associated with the toxic treatment of relapsed patients urge for a better and earlier identification of patients with occult metastatic disease. The SLN procedure could lead to less intensive follow-up protocols for node-negative patients and reduction of systemic treatment. In one study with a median follow-up of more than 5 years, none of the patients with a negative SLN suffered from relapse [69].

15.4.2 Indications and Contraindications for SLNB

SLN visualization is feasible in patients with clinical stage I disease [69, 70, 82, 83]. Clinical stage I is defined by the absence of enlarged (>1 cm) lymph nodes on abdomino-thoracic computed tomography (CT) scan plus normal or normalizing serum values of alpha-fetoprotein (AFP), human chorionic gonadotropin (HCG), and lactate dehydrogenase (LDH).

15.4.3 Radiocolloid and Modalities of Injection

The route of administration of ^{99m}Tc-nanocolloid has been evaluated in multiple feasibility studies. While funicular administration showed only lymph node uptake in the inguinal region (which does not reflect the actual testicular tumor drainage pattern), intratesticular administration resulted in visualization of retroperitoneal SLNs, in accordance with known drainage patterns. No side effects were observed using the latter method, which proved to be easy to perform and was well tolerated under local anesthesia (funicular block with lidocaine 2%). Generally, a single aliquot of radioactivity (approximately 100 MBq) in a volume of 0.1–0.2 mL is injected with a fine needle into the testicular parenchyma.

15.4.4 Preoperative Imaging of SLNs

The fast lymphatic drainage from the testicle requires dynamic gamma camera acquisition to facilitate differentiation between first- and second-echelon lymph nodes in the retroperitoneum. Immediately following radiocolloid injection, anterior and lateral dynamic images are obtained with a dual-head gamma camera to visualize the lymphatic flow and early-draining lymph nodes. Static planar images are obtained immediately after the dynamic study. Two hours after tracer injection, additional static images are obtained to identify slower draining SLNs and unexpected drainage patterns.

15.4.5 Lymphatic Drainage

Left-sided testicular tumors primarily drain to the para-aortic retroperitoneal region [84]. Right-sided tumors show a less uniform pattern of dissemination and drain to the paracaval, precaval, and interaortocaval region [84, 85].

15.4.6 Intraoperative Detection of SLNs

SLNB in testicular cancer was introduced in a laparoscopic setting, and can also be performed robot assisted. Intraoperative SLN localization is guided by a laparoscopic gamma probe or a portable gamma camera [69, 71].

15.4.7 Contribution of SPECT/CT

In the initial feasibility study, preoperative lymphatic mapping was performed using planar lymphoscintigraphy only [70]. However, this technique can provide two-dimensional information only, and exact preoperative anatomical SLN localization is not possible. SPECT/CT provides not only useful anatomic information about the location of SLNs but its improved sensitivity and the added third dimension may also lead to the detection of additional SLNs (Fig. 15.8). Sequential planar imaging will remain important for the preoperative identification of early-appearing lymph nodes as SLNs.

15.4.8 Intraoperative Imaging

Since the lymphatic drainage of the testes is directed to retroperitoneal areas deeply within the abdomen that can often

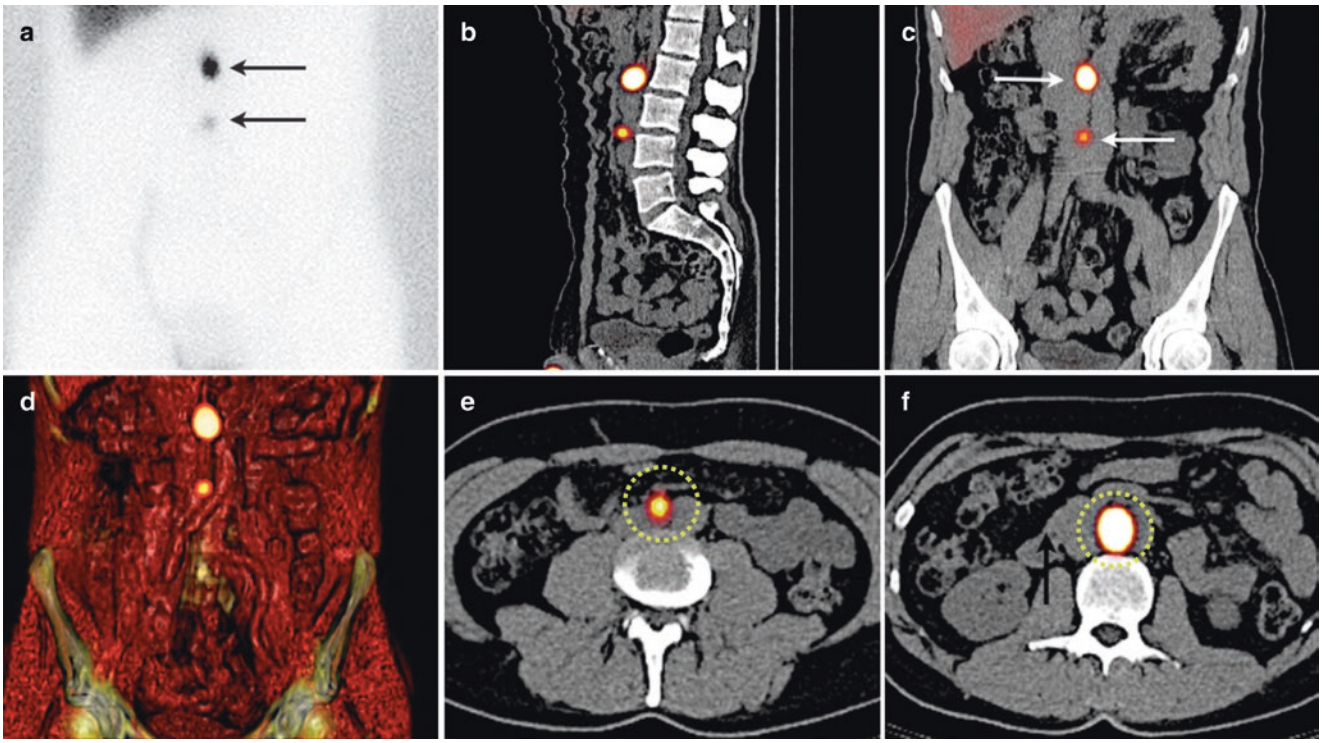

Fig. 15.9 A 42-year-old male with a seminoma in the right testicle was injected with ^{99m}Tc-nanocolloid (87.32 MBq) followed by SLN mapping. (**a**) Early planar anterior image showing drainage to two abdominal SLNs (arrows) and radioactivity along the lymphatic channel, which decreased in time, indicating lymphatic tract visualization. (**b**) Sagittal SPECT/CT image fusion showing the injection site and both SLNs along the great abdominal vessels. (**c**, **d**) The coronal SPECT/CT image fusion and 3D volume-rendered image reveal that both SLNs are located interaortocavally (arrows). (**e**, **f**) Axial SPECT/CT images providing additional anatomical information about the location of both SLNs (dotted circles). Both SLNs were harvested laparoscopically and were tumor free at histopathology

be complex, preoperative anatomical information about the location of the SLNs is important for planning the surgical procedure. For this reason, the SPECT/CT images should be displayed in the operating room. Urological surgery has shifted from the open approach toward minimally invasive laparoscopic and robot-assisted techniques. During laparoscopic surgery, the urologist localizes a SLN under guidance by the sound pitch from the laparoscopic gamma probe. However, intraoperative spatial orientation using this device can be difficult, as a laparoscopic probe does not provide visual information. The use of a portable gamma camera helps to intraoperatively guide laparoscopic SLN localization as described above (see section *Intraoperative detection of SLNs: prostate cancer*). This approach provides certainty about completeness of the surgical procedure and complements the laparoscopic probe. Currently, intraoperative navigation approaches that are based on the preoperative (SPECT/CT) images are being developed [86].

15.4.9 Common and Rare Variants

Although drainage from the testes is usually directed to paracaval, interaortocaval, and para-aortic SLNs, in some patients SLNs may also be seen along the testicular vessels (Fig. 15.9) [71].

15.4.10 Technical Pitfalls

The route of administration of ^{99m}Tc-nanocolloid may cause pitfalls. For instance, funicular administration may result in lymph node uptake in the inguinal region, which does not reflect testicular tumor drainage. Intratesticular administration in the parenchyma results in retroperitoneal SLN visualization, in accordance with known drainage patterns (Fig. 15.10).

15.4.11 Accuracy of Radioguided SLNB

To date, no studies have been published other than the aforementioned feasibility studies limited by small size of the study populations (~25 patients per study). Although refinement of the SLN procedure may enable better selection of patients who would benefit from adjuvant treatment after orchidectomy, further studies are required to substantiate the clinical value of the SLNs procedure in this disease.

Key Learning Points: Testicular Cancer

- Occult metastatic disease is common in clinical stage I testicular cancer and has serious implications for these relatively young patients.
- Lymphatic mapping using lymphoscintigraphy and SPECT/CT is essential to localize SLNs, by providing specific anatomical landmarks for subsequent surgical resection.
- The SLN procedure could lead to less intensive follow-up protocols and reduction of systemic treatment.
- Larger, prospective studies are necessary to evaluate the role of the SLN procedure in testicular cancer.

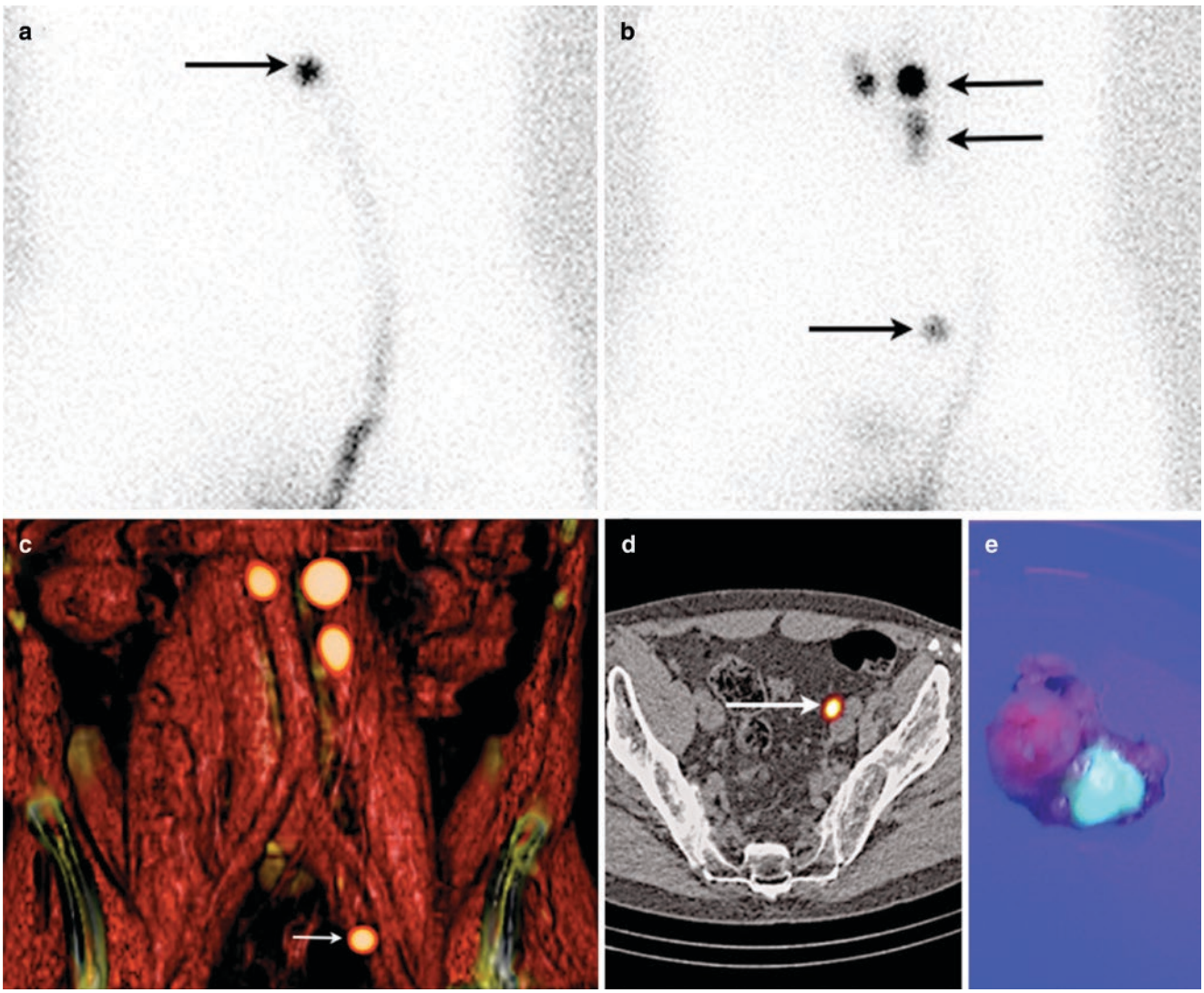

Fig. 15.10 Intratesticular injection of hybrid ICG-^{99m}Tc-nanocolloid (67.7 MBq) in a 52-year-old male with a seminoma in his left testicle followed by lymphoscintigraphy and SPECT/CT. (**a**) Early planar anterior image showing drainage from the left testicle toward an abdominal SLN (arrow). (**b**) The delayed lymphoscintigram reveals an additional SLN just below the SLN which was visualized on the early image (upper arrows), a second-echelon node to the right, and an additional hot spot located more caudally (lower arrow) which was therefore also defined as SLN. (**c**) Fused SPECT/CT image displayed with 3D volume rendering showing the cranial two SLNs alongside the aorta, the interaortocaval second-echelon node, and the more caudal SLN (arrow) next to the funiculus. (**d**) Axial fused SPECT/CT image depicting the caudal SLN along the external iliac vessels next to the funiculus. All SLNs were excised during laparoscopy guided by a laparoscopic gamma probe and fluorescence endoscope. (**e**) Ex vivo fluorescence image of a para-aortal SLN revealing the location of the node within the excised tissue specimen

Clinical Cases

Case 15.1: SLN Mapping in Penile Cancer with Bilateral Drainage to Both Groins

Renato A. Valdés Olmos, Henk G. van der Poel, and Oscar R. Brouwer

Background Clinical Case

A 78-year-old man with penile carcinoma was referred for SLNB. During staging of both groins no lymph node abnormalities had been detected on physical examination and ultrasonography (clinical stage T1N0).

Planar Lymphoscintigraphy and SPECT/CT Imaging

In the afternoon before surgery a total of 110 MBq ICG-^{99m}Tc-nanocolloid was administered in three intradermal injections proximal to the primary tumor into the glans. Immediately after tracer administration, a dynamic study was acquired during 10 min with the patient in supine position using a dual-head gamma camera (Symbia T, Siemens, Erlangen, Germany) equipped with low-energy high-resolution collimators. Subsequently, 5-min planar static images were acquired at 15 min and 2 h postinjection. In addition, SPECT/CT imaging was acquired after the 2-h delayed planar imaging using the same gamma camera.

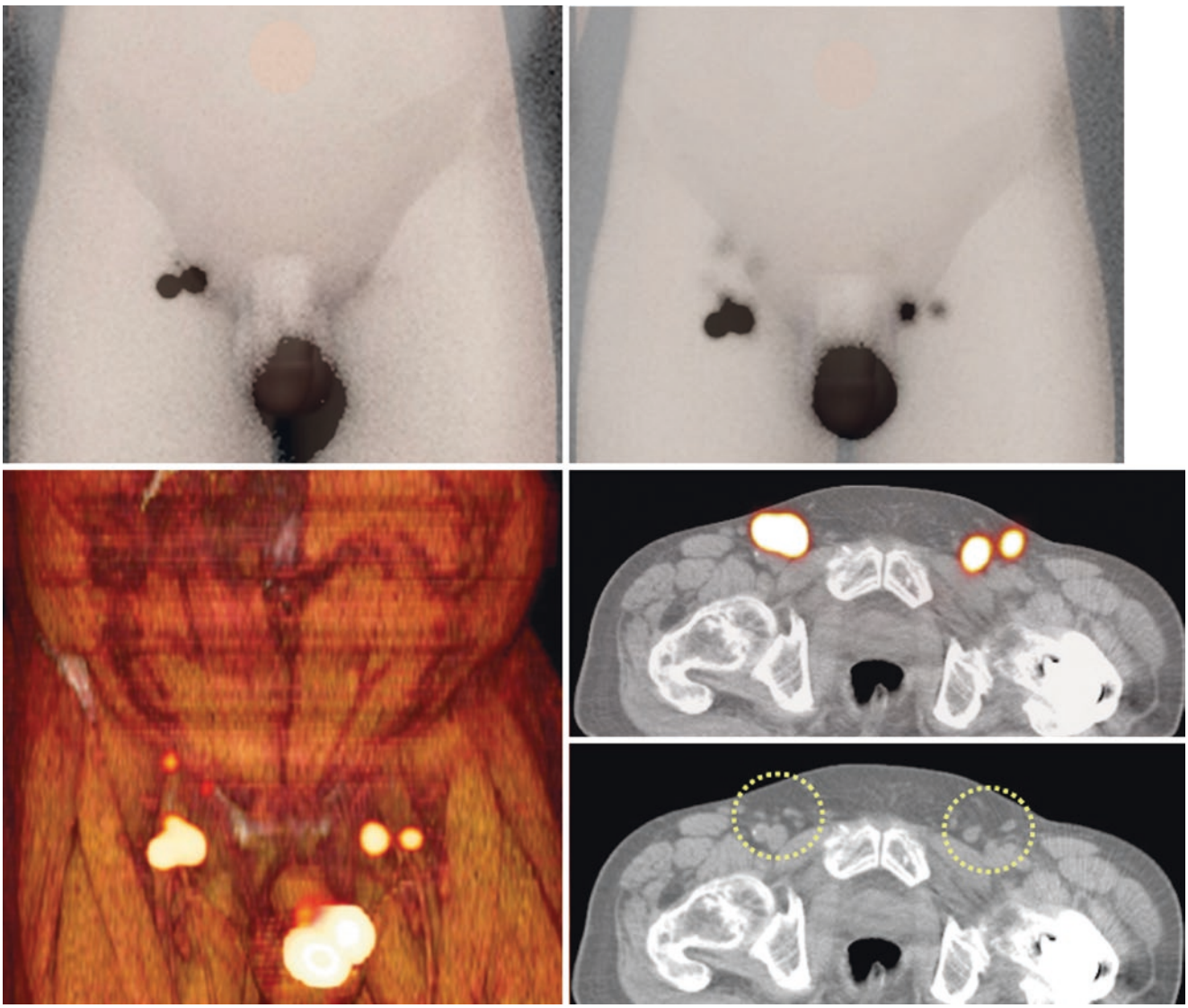

Fig. 15.11 Anterior early (on the left) and delayed (on the right) planar images, displayed in superposition to anatomical models, showing bilateral drainage to both groins. Inguinal SLNs in the left groin become clear only on delayed images. On SPECT/CT (bottom) radioactive SLNs in both groins are located above the saphenofemoral junction corresponding on low-dose CT to normal-size lymph nodes in the so-called upper inguinal zones of Daseler (circles)

Case 15.2: SLN Mapping in Recurrent Penile Carcinoma with Drainage to Iliac and Inguinal Lymph Nodes

Renato A. Valdés Olmos, Henk G. van der Poel, and Oscar R. Brouwer

Background Clinical Case

A 57-year-old man with a squamous-cell penile carcinoma recurrence was referred for SLNB. The patient had undergone partial penis amputation 13 years earlier because of a primary penile carcinoma (cT2N0) with subsequent lymph node dissection of the right groin due to SLN metastases (pT2N1). The SLN of the left groin at that time was free of tumor and no further surgical intervention had been performed. Following confirmation of the recurrence, no lymph node abnormalities had been detected on palpation and ultrasonography.

Planar Lymphoscintigraphy and SPECT/CT Imaging

In the afternoon before surgery a total of 100 MBq ICG-^{99m}Tc-nanocolloid was administered in three intradermal injections around the tumor recurrence following preparation with xylocaine 10% spray for local anesthesia. Immediately after tracer administration, a dynamic study was acquired during 10 min with the patient in supine position using a dual-head gamma camera (Symbia T, Siemens, Erlangen, Germany) equipped with low-energy high-resolution collimators. Subsequently, 5-min planar static images were acquired at 15 min and 2 h postinjection. In addition, SPECT/CT imaging was acquired after acquiring the delayed planar images using the same gamma camera.

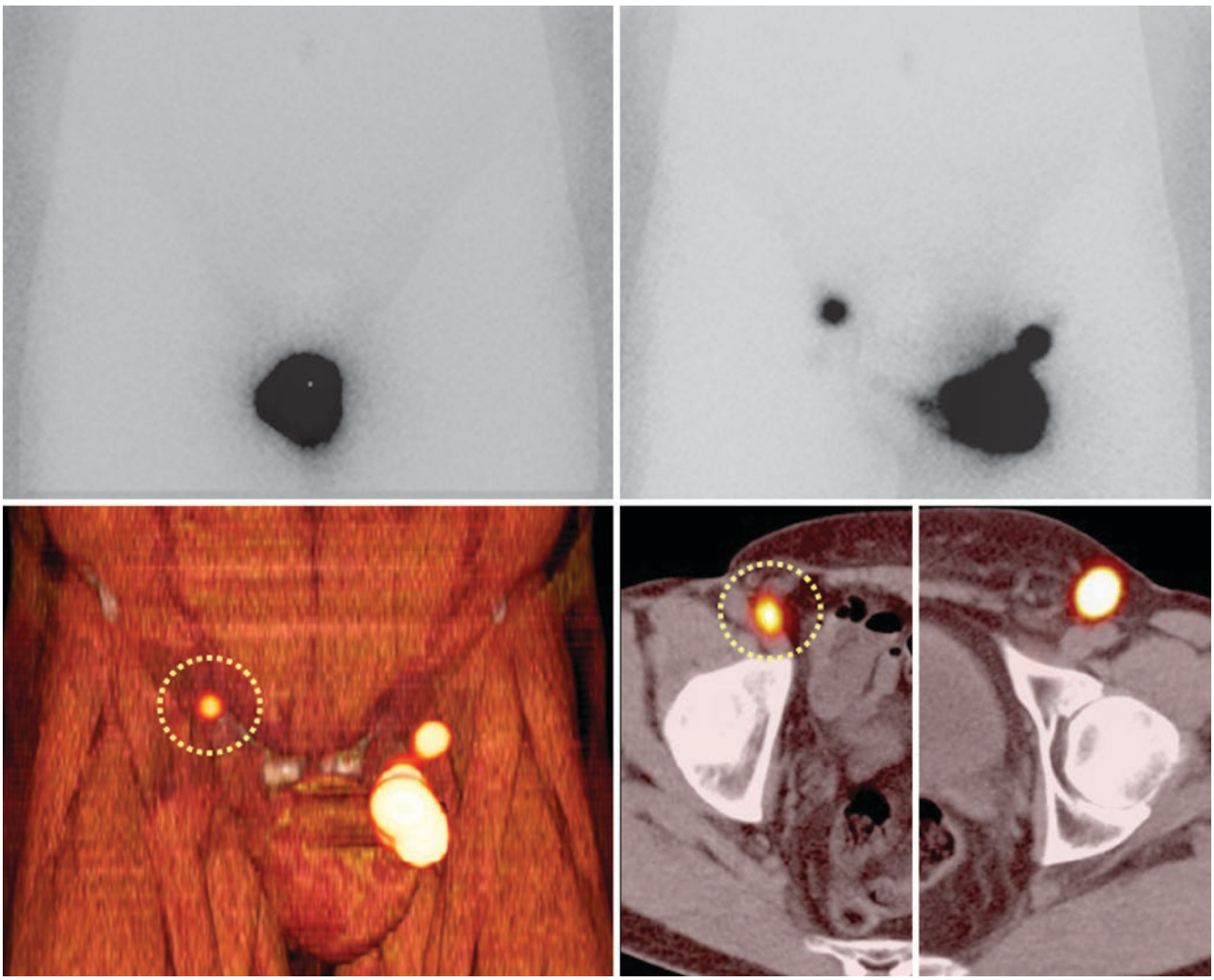

Fig. 15.12 Anterior static planar images displayed in superposition to anatomical models (upper row). Bilateral tracer migration to lymph nodes is only seen on delayed image (on the right) with a radioactive left lymph node near the penile injection site and a higher located node with a visible lymphatic duct in the right side. Note on SPECT/CT imaging (lower row) that the SLN in the right side is located in the vicinity of the external iliac artery (circles), whereas the SLN in the left side is located in the groin

Case 15.3: SLN Mapping in Prostate Carcinoma with Bilateral Drainage to Pelvic Lymph Nodes

Renato A. Valdés Olmos, Henk G. van der Poel, and Oscar R. Brouwer

Background Clinical Case

A 70-year-old man with confirmed carcinoma in the right lobe of the prostate on histopathology and Gleason 7 was referred for a SLN procedure with robot-assisted surgery. No lymph node abnormalities had been detected on radiological examination (clinical stage T2N0).

Planar Lymphoscintigraphy and SPECT/CT Imaging

The patient was planned for a 1-day SLN procedure. Early in the morning a total of 125 MBq ICG-^{99m}Tc-nanocolloid was administered in both lobes of the prostate by means of four injections guided by transrectal ultrasonography. Immediately after tracer administration, the patient was transferred to the department of nuclear medicine and a static image was acquired during 5 min with the patient in supine position using a dual-head gamma camera (Symbia T, Siemens, Erlangen, Germany) equipped with low-energy high-resolution collimators. Subsequently, delayed static images were acquired at 2 h postinjection. In addition, SPECT/CT imaging was acquired after acquiring the delayed planar images using the same gamma camera.

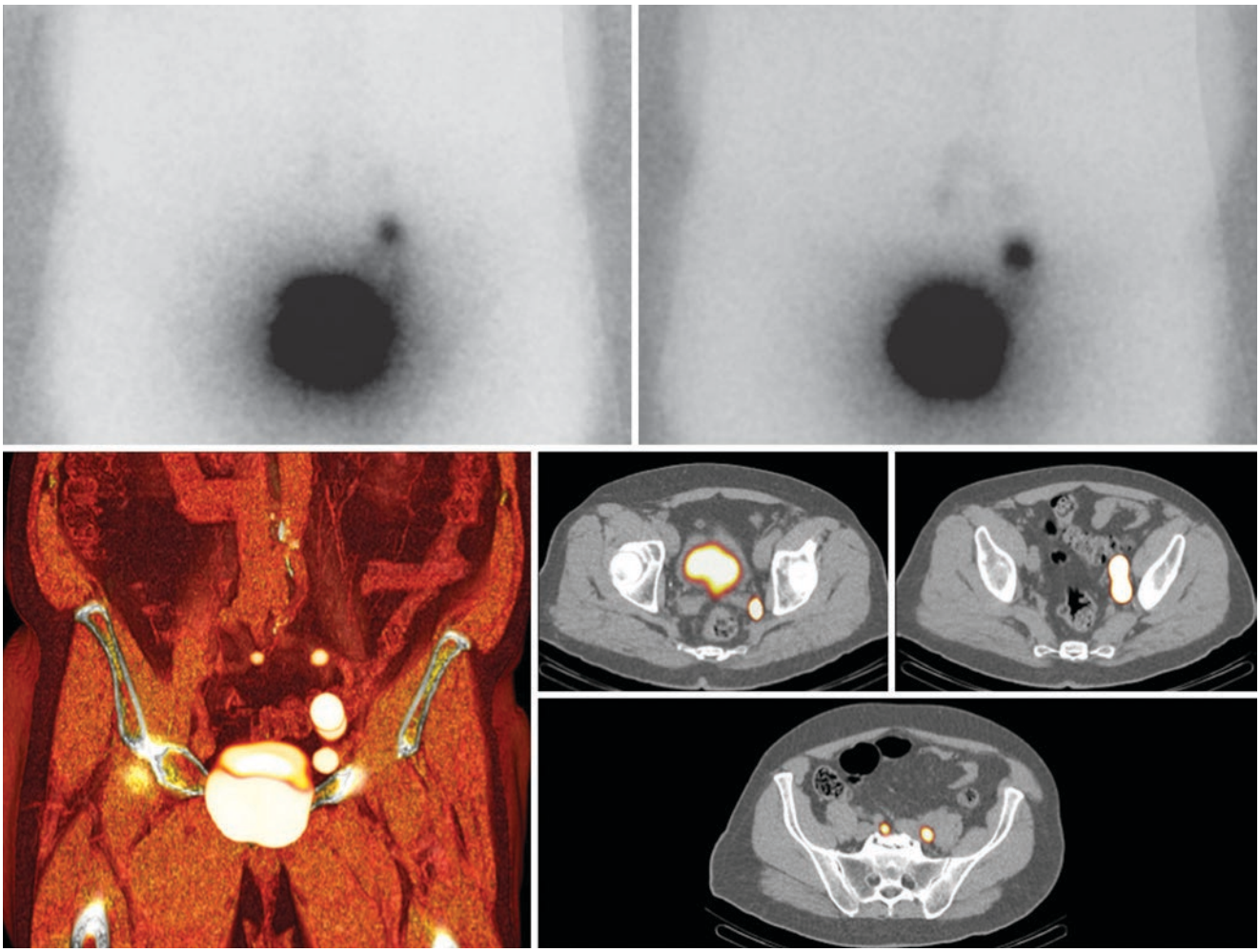

Fig. 15.13 Static planar images (upper row) are displayed in superposition to anatomical models. On early anterior (first frame) and right lateral (second frame) views bilateral lymph node uptake is seen principally on the left side of the pelvis. Volume-rendering and cross-sectional SPECT/CT images (lower row) show four SLNs along the left internal and common iliac arteries, whereas on the right side of the pelvis the SLN is located medially from the right common iliac vessels

Case 15.4: SLN Mapping in Prostate Carcinoma with Unilateral Drainage to a Pelvic Lymph Node

Renato A. Valdés Olmos, Henk G. van der Poel, and Oscar R. Brouwer

Background Clinical Case

A 70-year-old man with confirmed carcinoma in both lobes of the prostate on histopathology was referred for a SLN procedure with robot-assisted surgery. No lymph node abnormalities had been detected on radiological examination (clinical stage T2N0).

Planar Lymphoscintigraphy and SPECT/CT Imaging

Since a 1-day SLN procedure had been planned, the patient received in the morning a total of 115 MBq ICG-^{99m}Tc-nanocolloid by means of four injections in both lobes of the prostate guided by transrectal ultrasonography. Immediately after tracer administration, the patient was moved to the department of nuclear medicine and static 5-min images were acquired at 15 min and 2 h postinjection with the patient in supine position using a dual-head gamma camera (Symbia T, Siemens, Erlangen, Germany) equipped with low-energy high-resolution collimators. Subsequently to delayed static images, SPECT/CT imaging was acquired using the same gamma camera.

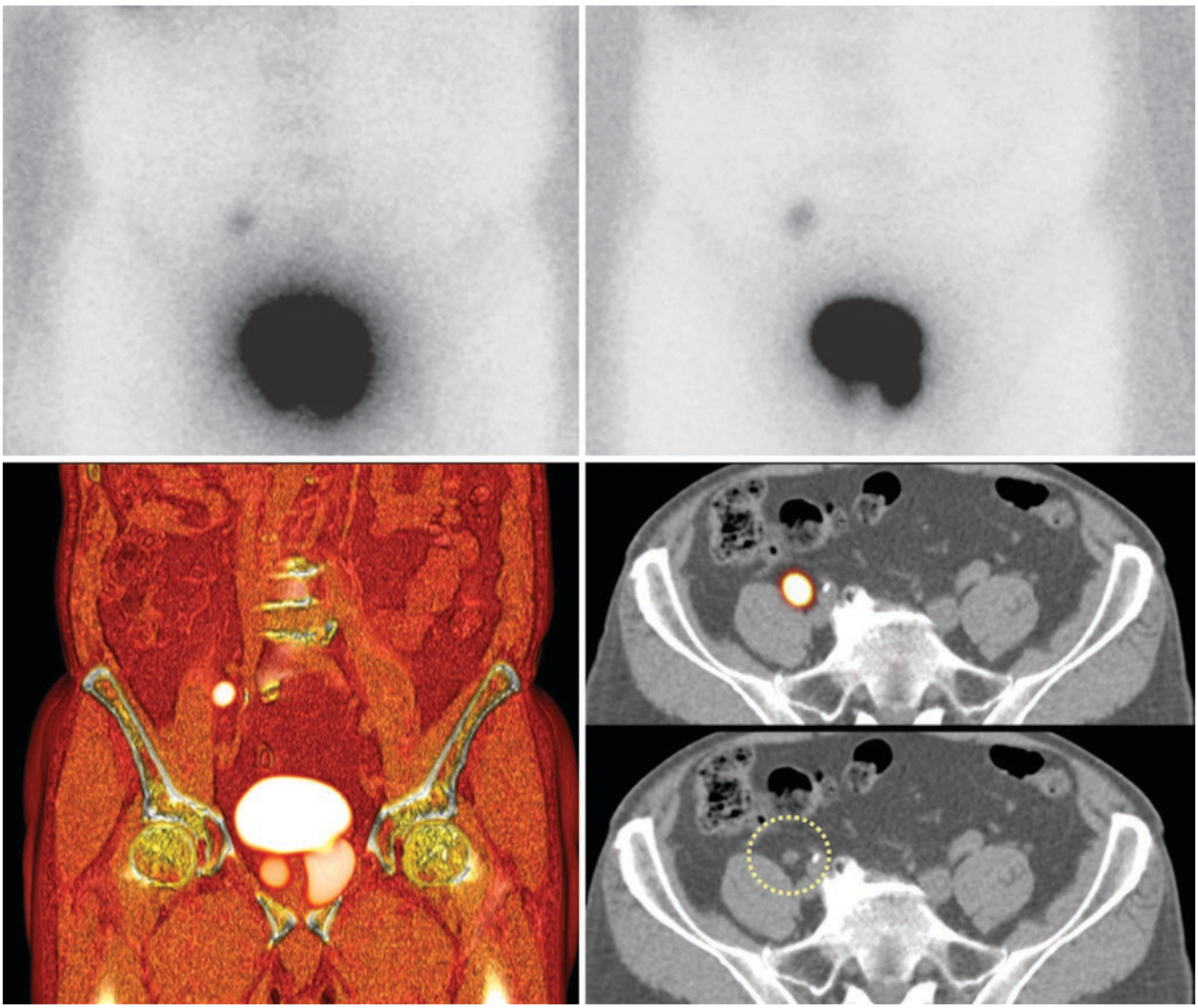

Fig. 15.14 Both early and delayed planar images (upper row), displayed in superposition to anatomical models, show migration of the tracer to the right side of the pelvis. Volume-rendering and cross-sectional SPECT/CT images (lower row) show one single SLN located laterally from the right common iliac vessels. The corresponding lymph node on low-dose CT (circle) is not enlarged

Case 15.5: SLN Mapping in Prostate Carcinoma with Drainage to Presacral and Mesorectal Lymph Nodes

Renato A. Valdés Olmos, Henk G. van der Poel, and Oscar R. Brouwer

Background Clinical Case

A 67-year-old man with carcinoma in both lobes of the prostate was referred for SLN procedure with robot-assisted surgery. No lymph node abnormalities had been detected on radiological examination (clinical stage T2N0).

Planar Lymphoscintigraphy and SPECT/CT Imaging

The procedure was based on a 1-day SLN procedure. Early in the morning the patient received a total of 120 MBq ICG-^{99m}Tc-nanocolloid by means of four injections in both lobes of the prostate guided by transrectal ultrasonography. Immediately after tracer administration, the patient was moved to the department of nuclear medicine and static 5-min images were acquired at 15 min and 2 h postinjection with the patient in supine position using a dual-head gamma camera (Symbia T, Siemens, Erlangen, Germany) equipped with low-energy high-resolution collimators. Subsequently to delayed static imaging, SPECT/CT imaging was acquired using the same gamma camera.

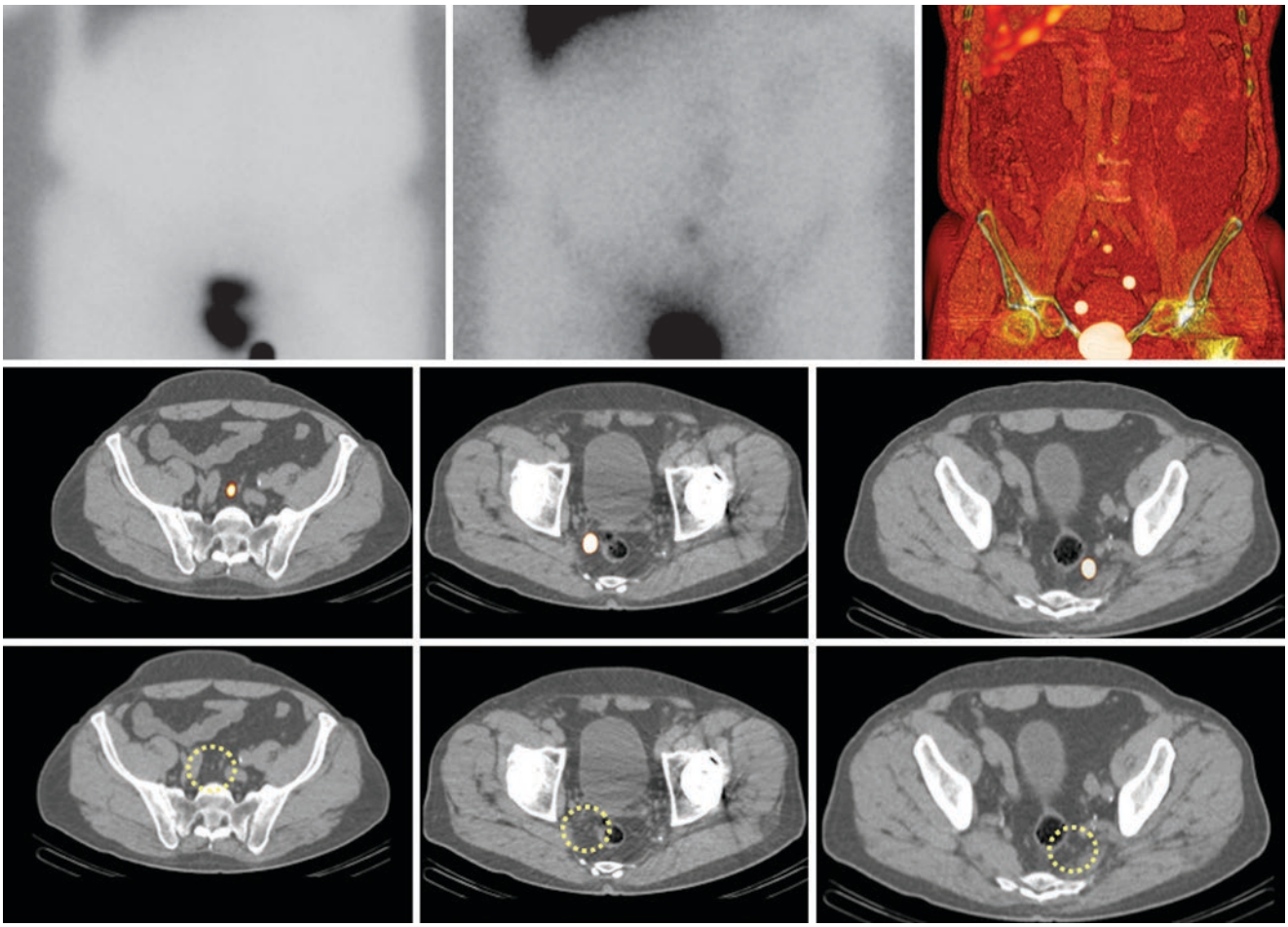

Fig. 15.15 Both early and delayed planar images (first two images in upper row), displayed in superposition to anatomical models, show delayed migration of the tracer to both sides of the pelvis. On volume-rendering SPECT/CT (last frame in upper row) the drainage becomes clearer, with visualization of three SLNs. Cross-sectional SPECT/CT images (lower row) show presacral and mesorectal SLNs. These radioactive nodes correspond to normal-size lymph nodes on low-dose CT (circles)

Case 15.6: SLN Mapping in Left Testicular Cancer with Unilateral Drainage to Para-aortic, Funicular, Iliac, and Inguinal Lymph Nodes

Renato A. Valdés Olmos, Henk G. van der Poel, and Oscar R. Brouwer

Background Clinical Case

A 35-year-old man with left testicle cancer was referred for SLN procedure. No lymph node abnormalities had been detected on radiological examination (clinical stage I).

Planar Lymphoscintigraphy and SPECT/CT Imaging

The day before surgery the patient received a total of 100 MBq ICG-^{99m}Tc-nanocolloid by means of a single injection in the left testicle in the proximity of the primary tumor following funicular block with 2% lidocaine. Immediately after tracer administration, a dynamic study was started during 10 min. Subsequently, static 5-min images were acquired at 15 min and 2 h postinjection with the patient in supine position using a dual-head gamma camera (Symbia T, Siemens, Erlangen, Germany) equipped with low-energy high-resolution collimators. Subsequently to delayed static images, SPECT/CT imaging was acquired using the same gamma camera.

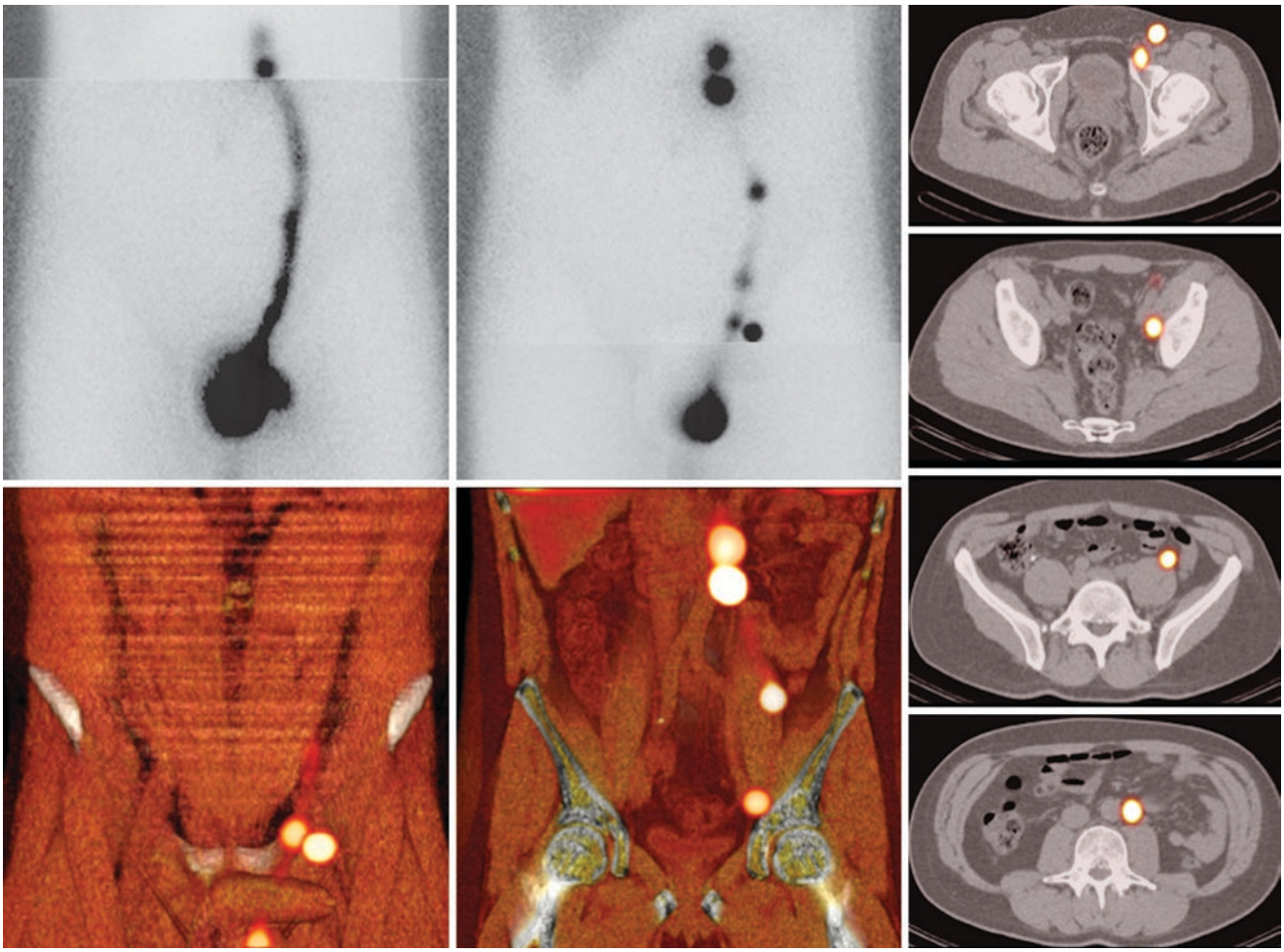

Fig. 15.16 Anterior planar images (first two images in upper row) are displayed in superposition to anatomical figures. Early static image (on the left) shows migration of the tracer from the left testicle through a long lymphatic vessel whereas delayed lymph node uptake is observed (second image) at various levels of pelvis and abdomen. On volume-rendering SPECT/CT (lower row) superficial (left image) and deep (second image) are displayed. Cross-sectional SPECT/CT images (right column) show inguinal and external iliac (top) as well as obturator and funicular SLNs (middle images) whereas the most cranial located lymph node is para-aortic (bottom)

Case 15.7: SLN Mapping in Right Testicular Cancer with Unilateral Drainage to Lymph Nodes Along the Vena Cava Inferior

Renato A. Valdés Olmos, Henk G. van der Poel, and Oscar R. Brouwer

Background Clinical Case

A 46-year-old man with right testicular cancer was referred for SLN procedure. No lymph node abnormalities had been detected on radiological examination (clinical stage I).

Planar Lymphoscintigraphy and SPECT/CT Imaging

The day before surgery the patient received a total of 90 MBq ^{99m}Tc-nanocolloid by means of a single injection in the right testicle in the vicinity of the primary tumor following funicular block with 2% lidocaine. Immediately after tracer administration a dynamic study was started during 10 min. Subsequently, static 5-min images were acquired at 15 min and 2 h postinjection with the patient in supine position using a dual-head gamma camera (Symbia T, Siemens, Erlangen, Germany) equipped with low-energy high-resolution collimators. Subsequently to delayed static images, SPECT/CT imaging was acquired using the same gamma camera.

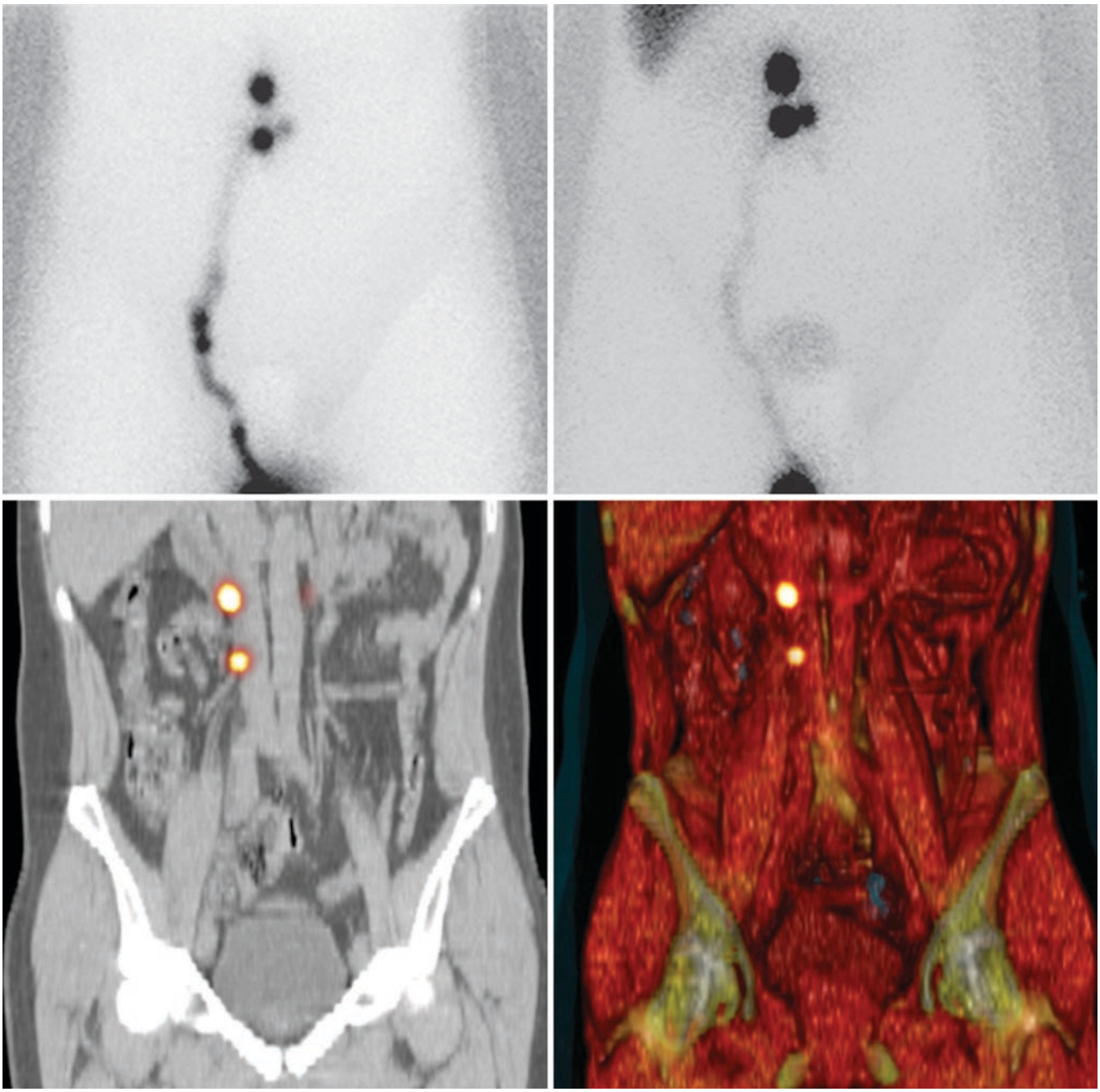

Fig. 15.17 Anterior planar images (upper row) are displayed in superposition to anatomical models. Early static image (on the left) shows migration of the tracer from the right testicle through a long lymphatic vessel with uptake in two lymph nodes. Delayed planar image (on the right) shows increasing uptake in the first draining lymph nodes and in a second echelon more medially located. On SPECT/CT imaging (lower row) both SLNs are seen laterally from the vena cava inferior

References

1. Van Den Berg NS, Van Leeuwen FWB, Van Der Poel HG. Fluorescence guidance in urologic surgery. Curr Opin Urol. 2012;22:109–20.
2. Brouwer OR, Buckle T, Vermeeren L, et al. Comparing the hybrid fluorescent-radioactive tracer indocyanine green-99mTc-nanocolloid with 99mTc-nanocolloid for sentinel node identification: a validation study using lymphoscintigraphy and SPECT/CT. J Nucl Med. 2012;53:1034–40.
3. Kleinjan GH, Van Den Berg NS, Brouwer OR, et al. Optimisation of fluorescence guidance during robot-assisted laparoscopic sentinel node biopsy for prostate cancer. Eur Urol. 2014;66:991–8.
4. Hernandez BY, Barnholtz-Sloan J, German RR, et al. Burden of invasive squamous cell carcinoma of the penis in the United States, 1998-2003. Cancer. 2008;113:2883–91.
5. Horenblas S, van Tinteren H. Squamous cell carcinoma of the penis. IV. Prognostic factors of survival: analysis of tumor, nodes and metastasis classification system. J Urol. 1994;151:1239–43.
6. Djajadiningrat RS, Graafland NM, van Werkhoven E, et al. Contemporary management of regional nodes in penile cancer-improvement of survival? J Urol. 2014;191:68–73.
7. Leijte JAP, Hughes B, Graafland NM, et al. Two-center evaluation of dynamic sentinel node biopsy for squamous cell carcinoma of the penis. J Clin Oncol. 2009;27:3325–9.
8. Kirrander P, Andrén O, Windahl T. Dynamic sentinel node biopsy in penile cancer: initial experiences at a Swedish Referral Centre. BJU Int. 2013;111:E48–53.
9. Lam W, Alnajjar HM, La-Touche S, et al. Dynamic sentinel lymph node biopsy in patients with invasive squamous cell carcinoma of the penis: a prospective study of the long-term outcome of 500 inguinal basins assessed at a single institution. Eur Urol. 2013;63:657–63.
10. Jakobsen JK, Krarup KP, Sommer P, et al. DaPeCa-1: diagnostic accuracy of sentinel lymph node biopsy in 222 patients with penile cancer at four tertiary referral centres - a national study from Denmark. BJU Int. 2016;117:235–43.
11. Dimopoulos P, Christopoulos P, Shilito S, et al. Dynamic sentinel lymph node biopsy for penile cancer: a comparison between 1- and 2-day protocols. BJU Int. 2016;117:890–6.
12. Stuiver MM, Djajadiningrat RS, Graafland NM, et al. Early wound complications after inguinal lymphadenectomy in penile cancer: a historical cohort study and risk-factor analysis. Eur Urol. 2013;64:486–92.
13. Spiess PE, Hernandez MS, Pettaway CA. Contemporary inguinal lymph node dissection: minimizing complications. World J Urol. 2009;27:205–12.
14. Hughes B, Leijte J, Shabbir M, et al. Non-invasive and minimally invasive staging of regional lymph nodes in penile cancer. World J Urol. 2009;27:197–203.
15. Woldu SL, Ci B, Hutchinson RC, et al. Usage and survival implications of surgical staging of inguinal lymph nodes in intermediate- to high-risk, clinical localized penile cancer: a propensity-score matched analysis. Urol Oncol. 2018;36:159.e7–159.e17.
16. Kroon BK, Horenblas S, Meinhardt W, et al. Dynamic sentinel node biopsy in penile carcinoma: evaluation of 10 years experience. Eur Urol. 2005;47:601–6.
17. Sadeghi R, Gholami H, Zakavi SR, et al. Accuracy of sentinel lymph node biopsy for inguinal lymph node staging of penile squamous cell carcinoma: systematic review and meta-analysis of the literature. J Urol. 2012;187:25–31.
18. TW Flaig PES. NCCN penile cancer 2018; 2018.
19. Hakenberg OW, Comperat E, Minhas S, et al. EAU guidelines penile cancer 2018; 2018.
20. Kroon BK, Horenblas S, Deurloo EE, et al. Ultrasonography-guided fine-needle aspiration cytology before sentinel node biopsy in patients with penile carcinoma. BJU Int. 2005;95:517–20.
21. Jakobsen JK, Alslev L, Ipsen P, et al. DaPeCa-3: promising results of sentinel node biopsy combined with (18) F-fluorodeoxyglucose positron emission tomography/computed tomography in clinically lymph node-negative patients with penile cancer—a national study from Denmark. BJU Int. 2016;118:102–11.
22. Lutzen U, Zuhayra M, Marx M, et al. Value and efficiency of sentinel lymph node diagnostics in patients with penile carcinoma with palpable inguinal lymph nodes as a new multimodal, minimally invasive approach. Eur J Nucl Med Mol Imaging. 2016;43:2313–23.
23. Graafland NM, Leijte JAP, Valdés Olmos RA, et al. Repeat dynamic sentinel node biopsy in locally recurrent penile carcinoma. BJU Int. 2010;105:1121–4.
24. Omorphos S, Saad Z, Arya M, et al. Feasibility of performing dynamic sentinel lymph node biopsy as a delayed procedure in penile cancer. World J Urol. 2016;34:329–35.
25. Kroon BK, Nieweg OE, van Boven H, et al. Size of metastasis in the sentinel node predicts additional nodal involvement in penile carcinoma. J Urol. 2006;176:105–8.
26. Kroon BK, Valdés Olmos RA, van Tinteren H, et al. Reproducibility of lymphoscintigraphy for lymphatic mapping in patients with penile carcinoma. J Urol. 2005;174:2214–7.
27. Winter A, Kowald T, Engels S, et al. Magnetic resonance sentinel lymph node imaging and magnetometer-guided intraoperative detection in penile cancer, using superparamagnetic iron oxide nanoparticles: first results. Urol Int. 2019:1–4.
28. Omorphos S, Saad Z, Kirkham A, et al. Zonal mapping of sentinel lymph nodes in penile cancer patients using fused SPECT/CT imaging and lymphoscintigraphy. Urol Oncol. 2018;36:530.e1–6.
29. Sahdev V, Albersen M, Christodoulidou M, et al. The management of non-visualisation following dynamic sentinel lymph node biopsy for squamous cell carcinoma of the penis. BJU Int. 2016;119:573–8.
30. Valdés Olmos RA, Tanis PJ, Hoefnagel CA, et al. Penile lymphoscintigraphy for sentinel node identification. Eur J Nucl Med. 2001;28:581–5.
31. Brouwer OR, van der Poel HG, Bevers RF, et al. Beyond penile cancer, is there a role for sentinel node biopsy in urological malignancies? Clin Transl Imaging. 2016;4:395–410.
32. Brouwer OR, Van Den Berg NS, Mathéron HM, et al. A hybrid radioactive and fluorescent tracer for sentinel node biopsy in penile carcinoma as a potential replacement for blue dye. Eur Urol. 2014;65:600–9.
33. Leijte JAP, van der Ploeg IMC, Valdés Olmos RA, et al. Visualization of tumor blockage and rerouting of lymphatic drainage in penile cancer patients by use of SPECT/CT. J Nucl Med. 2009;50:364–7.
34. Naumann CM, Colberg C, Jüptner M, et al. Evaluation of the diagnostic value of preoperative sentinel lymph node (SLN) imaging in penile carcinoma patients without palpable inguinal lymph nodes via single photon emission computed tomography/computed tomography (SPECT/CT) as compared to planar sci. Urol Oncol Semin Orig Investig. 2018;36:92.e17–24.
35. Saad ZZ, Omorphos S, Michopoulou S, et al. Investigating the role of SPECT/CT in dynamic sentinel lymph node biopsy for penile cancers. Eur J Nucl Med Mol Imaging. 2017;44:1176–84.
36. KleinJan GH, van Werkhoven E, van den Berg NS, et al. The best of both worlds: a hybrid approach for optimal pre- and intraoperative identification of sentinel lymph nodes. Eur J Nucl Med Mol Imaging. 2018;45:1915–25.
37. van Leeuwen AC, Buckle T, Bendle G, et al. Tracer-cocktail injections for combined pre- and intraoperative multimodal imaging of lymph nodes in a spontaneous mouse prostate tumor model. J Biomed Opt. 2011;16:016004.

38. Kroon BK, Valdés Olmos RA, van der Poel HG, et al. Prepubic sentinel node location in penile carcinoma. Clin Nucl Med. 2005;30:649–50.
39. Tanis PJ, Lont AP, Meinhardt W, et al. Dynamic sentinel node biopsy for penile cancer: reliability of a staging technique. J Urol. 2002;168:76–80.
40. Leijte JAP, Kroon BK, Valdés Olmos RA, et al. Reliability and safety of current dynamic sentinel node biopsy for penile carcinoma. Eur Urol. 2007;52:170–7.
41. Lont AP, Horenblas S, Tanis PJ, et al. Management of clinically node negative penile carcinoma: improved survival after the introduction of dynamic sentinel node biopsy. J Urol. 2003;170:783–6.
42. Zou Z-J, Liu Z-H, Tang L-Y, et al. Radiocolloid-based dynamic sentinel lymph node biopsy in penile cancer with clinically negative inguinal lymph node: an updated systematic review and meta-analysis. Int Urol Nephrol. 2016;48:2001–13.
43. Mottet N, Bellmunt J, Bolla M, et al. EAU-ESTRO-SIOG guidelines on prostate cancer. Part 1: screening, diagnosis, and local treatment with curative intent. Eur Urol. 2017;71(4):618–29.
44. Perera M, Papa N, Roberts M, et al. Gallium-68 prostate-specific membrane antigen positron emission tomography in advanced prostate cancer—updated diagnostic utility, sensitivity, specificity, and distribution of prostate-specific membrane antigen-avid lesions: a systematic review and meta-analysis. Eur Urol. 2020;77(4):403–17.
45. van Leeuwen PJ, Emmett L, Ho B, et al. Prospective evaluation of 68Gallium-prostate-specific membrane antigen positron emission tomography/computed tomography for preoperative lymph node staging in prostate cancer. BJU Int. 2017;119:209–15.
46. Meinhardt W, van der Poel HG, Valdés Olmos RA, et al. Laparoscopic sentinel lymph node biopsy for prostate cancer: the relevance of locations outside the extended dissection area. Prostate Cancer. 2012;2012:1–4.
47. Wit EMK, Acar C, Grivas N, et al. Sentinel node procedure in prostate cancer: a systematic review to assess diagnostic accuracy. Eur Urol. 2017;71:596–605.
48. Vermeeren L, Valdes Olmos RA, Meinhardt W, et al. Intraoperative imaging for sentinel node identification in prostate carcinoma: its use in combination with other techniques. J Nucl Med. 2011;52:741–4.
49. Meinhardt W. Sentinel node evaluation in prostate cancer. EAU-EBU Update Series. 2007;5:223–31.
50. Vermeeren L, Muller SH, Meinhardt W, et al. Optimizing the colloid particle concentration for improved preoperative and intraoperative image-guided detection of sentinel nodes in prostate cancer. Eur J Nucl Med Mol Imaging. 2010;37:1328–34.
51. de Bonilla-Damiá A, Roberto Brouwer O, Meinhardt W, et al. Lymphatic drainage in prostate carcinoma assessed by lymphoscintigraphy and SPECT/CT: its importance for the sentinel node procedure. Rev Esp Med Nucl Imagen Mol. 2012;31:66–70.
52. Joniau S, Van Den Bergh L, Lerut E, et al. Mapping of pelvic lymph node metastases in prostate cancer. Eur Urol. 2013;63:450–8
53. Van Den Bergh L, Joniau S, Haustermans K, et al. Reliability of sentinel node procedure for lymph node staging in prostate cancer patients at high risk for lymph node involvement. Acta Oncol (Madr). 2015;54:896–902.
54. van der Poel HG, Buckle T, Brouwer OR, et al. Intraoperative laparoscopic fluorescence guidance to the sentinel lymph node in prostate cancer patients: clinical proof of concept of an integrated functional imaging approach using a multimodal tracer. Eur Urol. 2011;60:826–33.
55. KleinJan GH, van den Berg NS, de Jong J, et al. Multimodal hybrid imaging agents for sentinel node mapping as a means to (re)connect nuclear medicine to advances made in robot-assisted surgery. Eur J Nucl Med Mol Imaging. 2016;43:1278–87.
56. Vermeeren L, Valdés Olmos RA, Meinhardt W, et al. Intraoperative radioguidance with a portable gamma camera: a novel technique for laparoscopic sentinel node localisation in urological malignancies. Eur J Nucl Med Mol Imaging. 2009;36:1029–36.
57. van Oosterom MN, Simon H, Mengus L, et al. Revolutionizing (robot-assisted) laparoscopic gamma tracing using a drop-in gamma probe technology. Am J Nucl Med Mol Imaging. 2016;6:1–17.
58. Meershoek P, van Oosterom MN, Simon H, et al. Robot-assisted laparoscopic surgery using DROP-IN radioguidance: first-in-human translation. Eur J Nucl Med Mol Imaging. 2019;46:49–53.
59. Vermeeren L, Valdés Olmos RA, Meinhardt W, et al. Value of SPECT/CT for detection and anatomic localization of sentinel lymph nodes before laparoscopic sentinel node lymphadenectomy in prostate carcinoma. J Nucl Med. 2009;50:865–70.
60. Holl G, Dorn R, Wengenmair H, et al. Validation of sentinel lymph node dissection in prostate cancer: experience in more than 2,000 patients. Eur J Nucl Med Mol Imaging. 2009;36:1377–82.
61. Meinhardt W, Valdés Olmos RA, Van Der Poel HG, et al. Laparoscopic sentinel node dissection for prostate carcinoma: technical and anatomical observations. BJU Int. 2008;102:714–7.
62. Rajpert-De Meyts E, McGlynn KA, Okamoto K, et al. Testicular germ cell tumours. Lancet. 2016;387:1762–74.
63. Nallu A, Mannuel HD, Hussain A. Testicular germ cell tumors. Curr Opin Oncol. 2013;25:266–72.
64. Trabert B, Chen J, Devesa SS, et al. International patterns and trends in testicular cancer incidence, overall and by histologic subtype, 1973-2007. Andrology. 2015;3:4–12.
65. Tandstad T, Smaaland R, Solberg A, et al. Management of seminomatous testicular cancer: a binational prospective population-based study from the Swedish Norwegian Testicular Cancer Study Group. J Clin Oncol. 2011;29:719–25.
66. Aparicio J, García del Muro X, Maroto P, et al. Multicenter study evaluating a dual policy of postorchiectomy surveillance and selective adjuvant single-agent carboplatin for patients with clinical stage I seminoma. Ann Oncol. 2003;14:867–72.
67. Kollmannsberger C, Moore C, Chi KN, et al. Non-risk-adapted surveillance for patients with stage I nonseminomatous testicular germ-cell tumors: diminishing treatment-related morbidity while maintaining efficacy. Ann Oncol. 2010;21:1296–301.
68. Powles TB, Bhardwa J, Shamash J, et al. The changing presentation of germ cell tumours of the testis between 1983 and 2002. BJU Int. 2005;95:1197–200.
69. Blok JM, Kerst JM, Vegt E, et al. Sentinel node biopsy in clinical stage I testicular cancer enables early detection of occult metastatic disease. BJU Int. 2019;124(3):424–30.
70. Tanis PJ, Horenblas S, Valdés Olmos RA, et al. Feasibility of sentinel node lymphoscintigraphy in stage I testicular cancer. Eur J Nucl Med. 2002;29:670–3.
71. Brouwer OR, Valdes Olmos RA, Vermeeren L, et al. SPECT/CT and a portable camera for image-guided laparoscopic sentinel node biopsy in testicular cancer. J Nucl Med. 2011;52:551–4.
72. Albers P, Albrecht W, Algaba F, et al. Guidelines on testicular cancer: 2015 update. Eur Urol. 2015;68:1054–68.
73. Kollmannsberger C, Tandstad T, Bedard PL, et al. Patterns of relapse in patients with clinical stage I testicular cancer managed with active surveillance. J Clin Oncol. 2015;33:51–7.
74. Pierorazio PM, Albers P, Black PC, et al. Non-risk-adapted surveillance for stage I testicular cancer: critical review and summary. Eur Urol. 2018;73:899–907.
75. Kerns SL, Fung C, Monahan PO, et al. Cumulative burden of morbidity among testicular cancer survivors after standard cisplatin-based chemotherapy: a multi-institutional study. J Clin Oncol. 2018;36:1505–12.
76. van den Belt-Dusebout AW, de Wit R, Gietema JA, et al. Treatment-specific risks of second malignancies and cardiovascular disease in 5-year survivors of testicular cancer. J Clin Oncol. 2007;25:4370–8.

77. Kvammen O, Myklebust TA, Solberg A, et al. Long-term relative survival after diagnosis of testicular germ cell tumor. Cancer Epidemiol Biomark Prev. 2016;25:773–9.
78. Warde P, Specht L, Horwich A, et al. Prognostic factors for relapse in stage I seminoma managed by surveillance: a pooled analysis. J Clin Oncol. 2002;20:4448–52.
79. Albers P, Siener R, Kliesch S, et al. Risk factors for relapse in clinical stage I nonseminomatous testicular germ cell tumors: results of the German Testicular Cancer Study Group Trial. J Clin Oncol. 2003;21:1505–12.
80. Lago-Hernandez CA, Feldman H, O'Donnell E, et al. A refined risk stratification scheme for clinical stage 1 NSGCT based on evaluation of both embryonal predominance and lymphovascular invasion. Ann Oncol. 2015;26:1396–401.
81. Klepp O, Dahl O, Flodgren P, et al. Risk-adapted treatment of clinical stage 1 non-seminoma testis cancer. Eur J Cancer. 1997;33:1038–44.
82. Ohyama C, Chiba Y, Yamazaki T, et al. Lymphatic mapping and gamma probe guided laparoscopic biopsy of sentinel lymph node in patients with clinical stage I testicular tumor. J Urol. 2002;168:1390–5.
83. Satoh M, Ito A, Kaiho Y, et al. Intraoperative, radio-guided sentinel lymph node mapping in laparoscopic lymph node dissection for stage I testicular carcinoma. Cancer. 2005;103:2067–72.
84. Weissbach L, Boedefeld EA. Localization of solitary and multiple metastases in stage II nonseminomatous testis tumor as basis for a modified staging lymph node dissection in stage I. J Urol. 1987;138:77–83.
85. Ray B, Hajdu SI, Whitmore WF. Distribution of retroperitoneal lymph node metastases in testicular germinal tumors. Cancer. 1974;33:340–8.
86. Brouwer OR, Buckle T, Bunschoten A, et al. Image navigation as a means to expand the boundaries of fluorescence-guided surgery. Phys Med Biol. 2012;57:3123–36.